

2018

INSTRUMENTATION OF MEASURING CELLULAR CAPACITANCE VIA SIGNAL PROCESSING TOOL

Mosa Al Zoweilei
University of Rhode Island, mosa1@uri.edu

Follow this and additional works at: <https://digitalcommons.uri.edu/theses>

Terms of Use

All rights reserved under copyright.

Recommended Citation

Al Zoweilei, Mosa, "INSTRUMENTATION OF MEASURING CELLULAR CAPACITANCE VIA SIGNAL PROCESSING TOOL" (2018). *Open Access Master's Theses*. Paper 1300.
<https://digitalcommons.uri.edu/theses/1300>

This Thesis is brought to you by the University of Rhode Island. It has been accepted for inclusion in Open Access Master's Theses by an authorized administrator of DigitalCommons@URI. For more information, please contact digitalcommons-group@uri.edu. For permission to reuse copyrighted content, contact the author directly.

INSTRUMENTATION OF MEASURING CELLULAR CAPACITANCE VIA SIGNAL

PROCESSING TOOL

BY

MOSA AL ZOWELEI

A THESIS SUBMITTED IN PARTIAL FULFILLMENT OF THE

REQUIREMENTS FOR THE DEGREE OF

MASTER OF SCIENCE

IN

ELECTRICAL ENGINEERING

SPECIALIZED IN BIOMEDICAL ENGINEERING

UNIVERSITY OF RHODE ISLAND

2018

MASTER OF SCIENCE THESIS

OF

MOSA AL ZOWELEI

APPROVED:

Thesis Committee:

Major Professor Ying Sun

John DiCecco

Feruz Ganikhanov

Nasser H. Zawia
DEAN OF THE GRADUATE SCHOOL

UNIVERSITY OF RHODE ISLAND
2018

ABSTRACT

This master thesis pertains to a systematic testing and evaluation of three neuroscience instruments previously developed at the Biomedical Engineering Laboratory of the University of Rhode Island. The three instruments are the Universal Clamp (UC), the Neuron Emulator (NE), and the Cell Capacitance Emulator (CCE). The UC is an innovative instrument that employs a fast-digital signal processor to deliver and integrate various experimental tools for electrophysiology. The NE is an electronic device that uses a capacitance source to represent the passive and active electrical properties of a neuron. The CCE presents a dynamic resistance-capacitance model of a neuron with the capability of switching between two capacitances that have a small difference to represent the activity of a vesicle crossing the cell membrane.

A platform for conducting a systematic testing on the functionality of the UC by use of the NE and the CCE was developed. The main objective was to explore the possibilities and drawbacks of using such a platform to test neuroscience instruments without the need for a wet experiment involving live neurons. The functions of the UC under evaluation included voltage clamp, current clamp, and cell capacitance measurement. The contributions of this research include the hardware and software improvements on the NE and CCE necessary for integrating them into the testing platform. An attempt to reduce of the rise time of the action potential spike by adding a low-pass filter at the output circuitry made the action potential waveform more realistic; however, the low-pass filter also reduced the speed for the feedback currents and resulted in an unsuccessful voltage clamp. The representation of the cell capacitance changes due to a vesicle activity on the order of 10 fF with a 2-ms pulse

width was challenging. The parasitic capacitance from the wiring and the breadboard was often on the order of 10 pF. The existing algorithm based on short-time Fourier transform for detecting the vesicle capacitance was insufficient to detect such a small and fast capacitance change.

In summary, this thesis research has demonstrated an instrumentation platform and testing methods for electrophysiological instruments using only electronic devices. While the system does not completely replace the need for using live neurons, many standard experimental protocols such as current clamp and voltage clamp can be tested in an efficient and effective way.

ACKNOWLEDGMENTS

The goal is to write a master's thesis to complete my Master of Science degree in Electrical engineering, specialized in Biomedical engineering. That goal along many other aims, I have had during the journey, would not be achieved without the generous support of many people.

I would like to thank all my family members mainly my parents, department of Electrical, Computer, and Biomedical Engineering, for all their ceaseless hard work and passion in both teaching and in research, while simultaneously encouraging their students to set and achieve exceptionally high goals.

Throughout my time here at the University, there has been one Professor who has been gracious and kind enough to believe in me and to allow me to work and study under him for few years, through independent studies, capstone project and master's thesis. It is with no exaggeration that I can say I would not be here right now, presenting this thesis, without the help and mentorship of Dr. Ying Sun. He has not only had a direct impact on my life, but on many other students who have had the privilege to pass through this wonderful program he started. With that, I extend my deepest and most heartfelt thank you to Dr. Ying Sun.

Last but certainly not least, I would like to thank my committee members who were great point of support for me through the journey as they were my professors of multiple classes and I have had the pleasure to work with some of them as an undergraduate teacher assistant for three years and a graduate assistant for a year. With that said, I extend my deepest and most heartfelt thank you to Dr. Peter Nightingale, Dr. John DiCecco, & Dr. Feruz Ganikhanov.

Finally, it is unrealistic to think I have acknowledged everyone who deserves the recognition including my URI career / student / residential / international students advisors, my friends and my classmates. This does not make your contributions towards me or your influence on my life any less substantial. I think you all know who you are and I thank you.

TABLE OF CONTENTS

ABSTRACT	ii
ACKNOWLEDGMENTS	iv
TABLE OF CONTENTS	vi
LIST OF TABLES	ix
LIST OF FIGURES	x
CHAPTER 1	1
INTRODUCTION	1
1.1 Executive summary.....	1
1.2 Review of the electrophysiology	1
1.3 Overview of experimental methods in electrophysiology	2
1.4 Value of simulating action potential vs biological experiment	4
1.5 List of references.....	5
CHAPTER 2	6
UNIVERSAL CLAMP	6
2.1 Introduction.....	6
2.2 Voltage Clamp	6
2.3 Current Clamp.....	8
2.4 Dynamic Clamp	8
2.5 Patch Clamp	8
2.6 Universal Clamp	10
2.7 List of References	10

CHAPTER 3	12
NEURON EMULATOR.....	12
3.1 Introduction.....	12
3.2 Neuron Emulator Innovation	13
3.3 Theory of Operation of the Neuro Emulator.....	14
3.4 Preliminary Testing Results	18
3.5 Attempt to Increase the Rise Time.....	20
3.5.1 Attempt to Increase the Switching Time	21
3.5.2 Adding a Low-Pass Filter at the Output	22
3.6 List of references.....	28
CHAPTER 4	29
CELL CAPACITANCE EMULATOR	29
4.1 Background.....	29
4.2 Introduction to the Cell Capacitance Emulator.....	29
4.3 Instrumentation of the Cell Capacitance Emulator	30
4.4 List of References	34
CHAPTER 5	36
METHODS FOR MEASURING CELL CAPACITANCES	36
5.1 Introduction.....	36
5.2 Existing Method.....	36
5.3 A Frequency-Domain Method	37
5.4 A Time-Domain Method.....	38
5.5 List of references.....	40

CHAPTER 6	42
SYSTEMATIC TESTING OF THE UNIVERSAL CLAMP	42
6.1 Introduction.....	42
6.2 Testing Setup	42
6.3 Ethernet Connection.....	44
6.4 Instrument Panel	47
6.5 Digital Filter Bank	52
6.6 Offset Voltage.....	53
6.7 Current Clamp.....	54
6.8 Voltage Clamp	57
6.9 Voltage Clamp With Neuron Emulator	59
6.10 Voltage Clamp With Modified Neuron Emulator	61
6.11 List of References	64
CHAPTER 7	65
TESTING OF CELL CAPACITANCE MEASUREMENTS	65
7.1 Instrumentation	65
7.2 Test Results.....	66
7.3 List of References	71
BIBLIOGRAPHY	72

LIST OF TABLES

TABLE	PAGE
Table 1 Operation modes for the Cell Capacitance Emulator	33
Table 2 Analog bandwidths for difference selected ranges of the capacitance meter (GLK Model 3000).....	70

LIST OF FIGURES

FIGURE	PAGE
Figure 1 Hodgkin & Huxley action potential simulation equation	5
Figure 2 Voltage clamp used by Hodgkin & Huxley in 1952	7
Figure 3 Patch clamp configurations.....	10
Figure 4 The circuit diagram of the neuron emulator	17
Figure 5 The switching of the Rap-Cap circuit in two stages	17
Figure 6 The squid giant axon with parameters from the work of Hodge and Huxley	18
Figure 7 Shows the switching signal.....	19
Figure 8 The result of a step clamp experiment with the neuron emulator.....	19
Figure 9 Waveforms of the NE output (CH1), voltage clamped result (CH2) and switching signal (CH3)t	20
Figure 10 Panel A: Instrumentation for testing the rise time of the analog switch (MC14016). Panel B: Result of using a square wave input. Panel C: Result of using a triangular wave input. Panel B: Result of using a sinusoidal wave input	22
Figure 11 Panel A: Original schematic diagram of the 2nd-generation NE. Panel B: Waveforms for the witching signals, Panel C: Modified schematic diagram by adding a low-pass filter at the output.....	24
Figure 12 The Neuron Emulator (NE) implemented on a breadboard	25
Figure 13 Action potentials generated by the original NE are shown on the left (panels A-C) at different time resolutions. Action potentials generated by the modified NE	

with the output low-pass filter are shown on the right (panels D-F) at different time resolute	27
Figure 14 The schematic diagram of the CCE and the instrumentation setup with the Universal Clamp and the capacitance meter	31
Figure 15 The Cell Capacitance Emulator (CCE) implemented on a breadboard.....	34
Figure 16 High-resolution membrane capacitance measurements for the study of exocytosis and endocytosis, adapted from Rituper et al. [2].....	37
Figure 17 illustrates the concept of a switching excitation with sinusoidally amplitude- modulated current injection and an induced voltage that has a sinusoidal envelope with a phase shift.....	39
Figure 18 an illustrative diagrammatic view of the system that measures electrical properties of a measurand by time-multiplexing the current injection and the voltage measurement via a single port. The measurand is modeled as a 3-element circuit with a resistor	39
Figure 19 Testing Setup	43
Figure 20 Back-panel view to illustrate the setup of the Universal Clamp	44
Figure 21 Instrument Panel	45
Figure 22 Passive Neuron Model & Headstage	46
Figure 23 Full-screen Instrument Panel	46
Figure 24 Instrument Panel	48
Figure 25 Digital Filter Bank	52
Figure 26 Filter with 1,000 Hz.....	53
Figure 27 Offset Voltage.....	54

Figure 28 current jumps to 10 nA and the voltage jumps to 20 mV	55
Figure 29 Message of current range setting	56
Figure 30 Injection a current pulse.....	57
Figure 31 Voltage Clamp Example.....	58
Figure 32 Voltage clamp on the passive neuron model with an increased Proportion gain (P=5.0), which resulted in a reduction of oscillation and a significant shorter settle time at the onset of the voltage clamp	59
Figure 33 Neuron Emulator circuit with the connection to the headstage.....	60
Figure 34 result of the voltage clamp experiment.....	61
Figure 35 Action potentials generated by the modified Neuron Emulator with a low-pass filter added to the output	62
Figure 36 Unsuccessful voltage clamp with the modified Neuron Emulator that has an added RC circuit at the output (Proportion gain = 1.0).....	63
Figure 37 Slightly improved voltage clamp with the modified Neuron Emulator that has an added RC circuit at the output (Proportion gain = 5.0).....	63
Figure 38 With a higher time resolution the delay of the feedback current can be observed	64
Figure 39 Block diagram of the instrumentation system for testing the cell capacitance measurements.....	65
Figure 40 Vesicle detection with the finger touching the passive neuron model	67
Figure 41 The present algorithm in the Universal Clamp failed to detect vesicle capacitance pulses with a 500 fA capacitance change and 1 500 mS pulse width	68

Figure 42 With a 10 nF capacitance difference, the Universal Clamp is capable of detecting the pulses with pulse width set to (left to right) 500 ms, 200 ms, 50 ms, and 2 ms, respectively..... 68

Figure 43 The capacitance meter (GLK Model 3000) is capable of detecting the 500 fF pulses with the 200 ms pulse width (left), but not with the 50 ms pulse width (right) 69

CHAPTER 1

INTRODUCTION

1.1 Executive summary

This master thesis is a systematic testing and evaluation of three products of Dr.Sun's BME lab. The three products are Universal Voltage clamp, Neuron Emulator, and Cell Capacitance Emulator. The universal clamp function has systematic integration tasks of the with Neuro Emulator as well as the cell capacitance, which would be covered in the thesis coming chapters. Hardware improvements are being applied for the success of the integrated testing, which will be also discussed in the coming chapters. The seven chapters are including introduction for the study and methodology of testing, Universal Voltage clamp, Neuron Emulator, Cell Capacitance Emulator, Methods for Measuring Cell Capacitances and the systemic testing which includes the integration and results of the evaluation as well as the hardware improvements.

1.2 Review of the electrophysiology

Electrophysiology is the study of the electrical properties of biological cells and tissues. It involves measurements of voltage changes or electric current or manipulations on a wide variety of scales from single ion channel proteins to whole organs like the heart. In neuroscience, it includes measurements of the electrical activity of neurons, and, in particular, action potential activity. Recordings of large-scale electric signals from the nervous system, such as electroencephalography (EEG), may also be referred to as electrophysiological recordings[1]. In BME lab at the University of Rhode Island, the founder (Dr. Ying Sun) and his team have added a major contribution to the

electrophysiology measurements by inventing what was called the universal voltage clamp. The new method, which would be discussed in details in the coming chapters, shows more accurate readings of capacitance across cell membranes. It is in a big favor of better diagnoses and measurements in electrophysiology.

1.3 Overview of experimental methods in electrophysiology

Electrophysiology is the branch of physiology that relates extensively to the stream of particles (particle current) in organic tissues and, specifically, to the electrical account procedures that empower the estimation of this stream. Established electrophysiology systems include putting cathodes into different arrangements of organic tissue. The chief sorts of terminals are:

1. simple strong conductors, for example, circles and needles (singles or clusters, regularly protected aside from the tip),
2. tracings on printed circuit sheets, likewise protected with the exception of the tip, and
3. hollow tubes loaded with an electrolyte, for example, glass pipettes loaded with potassium chloride arrangement or another electrolyte arrangement.

The key arrangements include:

1. living living beings,
2. excised tissue (intense or refined),
3. dissociated cells from extracted tissue (intense or refined),
4. artificially developed cells or tissues, or
5. hybrids of the above.

In the event that a terminal is sufficiently (micrometers) in width, at that point the electrophysiologist may embed the tip into a solitary cell. Such a setup permits coordinate

perception and recording of the intracellular electrical movement of a solitary cell. Be that as it may, this intrusive setup lessens the life of the cell and causes a break of substances over the cell film. Intracellular action may likewise be watched utilizing an uncommonly shaped (empty) glass pipette containing an electrolyte. In this system, the pipette tip is squeezed against the cell layer, to which it firmly follows by a cooperation amongst glass and lipids of the cell film. In the event that the tip is sufficiently little, such a setup may permit backhanded perception and recording of activity possibilities from a solitary cell, named single-unit recording. Contingent upon the readiness and exact arrangement, an extracellular setup may get the action of a few close-by cells all the while, named multi-unit recording.

To make an intracellular account, the tip of a fine (sharp) microelectrode must be embedded inside the cell, with the goal that the film potential can be estimated. Normally, the resting film capability of a sound cell will be - 60 to -80 mV, and amid an activity potential the layer potential may achieve +40 mV. In 1952, Hodgkin and Huxley showed understanding of the components hidden the age of activity possibilities in neurons. Their analyses included intracellular chronicles from the monster axon of Atlantic squid (*Loligo forbesi*) and were among the main uses of the "voltage cinch" strategy. Today, most microelectrodes utilized for intracellular account are glass micropipettes, with a tip measurement of < 1 micrometer, and an obstruction of a few megohms. The micropipettes are loaded with an answer that has a comparable ionic structure to the intracellular fluid of the cell. A chlorided silver wire embedded into the pipet interfaces the electrolyte electrically to the enhancer. The voltage estimated by the anode is contrasted with the voltage of a reference terminal, more often than not a silver

chloride-covered silver wire in contact with the extracellular liquid around the cell. The anode tip, the higher its electrical opposition, so a terminal is a trade off between estimate (sufficiently little to enter a solitary cell with least harm to the phone) and obstruction (sufficiently low so little neuronal signs can be perceived from warm commotion in the cathode tip).[2]

1.4 Value of simulating action potential vs biological experiment

Running biological experiments in engineering during initial design or research stages is unpractical. It requires the use of multiple resources. A simple biological experiment needs to be done in a safe lab environment with such high standards. Every time, a new experiment is being done takes time for set ups, more chemicals and different materials would be used which does increase the overall cost of the study. Moreover, it does have an ethical manner by affecting the environment while a better alternative is available.

On the other hand, the action potential simulation is efficient for the study. By using the Hodgkin & Huxley action potential simulation model, it takes few second to run an experiment. Also, there is no need of using different materials for each experiment. The Hodgkin & Huxley action potential simulation model is a set of nonlinear time-varying differential equation. (Please see Figure 1.1)

$$C_m \frac{dV}{dt} = -g_L (V - V_L) - \bar{g}_{Na} m^3 h (V - V_{Na}) - \bar{g}_K n^4 (V - V_K)$$

$$\frac{dm}{dt} = \alpha_m (V) (1 - m) - \beta_m (V) m$$

$$\frac{dh}{dt} = \alpha_h (V) (1 - h) - \beta_h (V) h$$

$$\frac{dn}{dt} = \alpha_n (V) (1 - n) - \beta_n (V) n$$

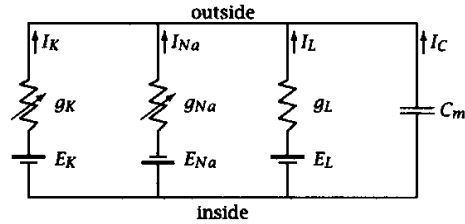


Figure 1 Hodgkin & Huxley action potential simulation equation

Figure is from Prof. Ying Sun*'s lab manual

*Biomedical engineering scientist and program director at the University of Rhode Island

As the figure shows, it is easily possible to predicate changes of voltage in a membrane.

[3]

Therefore, we are using the action potential simulation models in this study as it is the culture of the BME lab to consider environmental matters as major ethical manner.

1.5 List of references

1. Scanziani, Massimo; Häusser, Michael (2009). "Electrophysiology in the age of light". *Nature*. **461** (7266): 930–39.
2. Hodgkin & Huxley,(1952). ‘ The components of membrane conducted in the giant axon of Loligo.’ *Journal of Physiology*, 116, 473-496.
3. Hodgkin & Huxley,(1952). ‘ Currents carried by sodium and potassium ions through the membrane of the giant axon of Lologo .’ *Journal of Physiology*, 116, 449-472.

CHAPTER 2

UNIVERSAL CLAMP

2.1 Introduction

In this chapter, the Universal clamp is being discussed in detail along with electrophysiological methods including voltage clamp, current clamp, dynamic, and patch clamp and Patch clamp.

Universal Clamp is an innovative neuroscience instrument that has been developed in the Biomedical Engineering Lab at the University of Rhode Island. It has been awarded two US and international patents to date [1-2]. The Universal Clamp employs a high-speed digital signal processor to interact with the neurons. Under the software control, the Universal Clamp unifies and integrates the electrophysiological methods including voltage clamp, current clamp, dynamic clamp, and patch clamp.

2.2 Voltage Clamp

The voltage clamp strategy enables an experimenter to the cell voltage at a picked esteem. This makes it conceivable to gauge how much ionic current crosses a cell's layer at any given voltage. This is essential in light of the fact that huge numbers of the particle directs in the film of a neuron are voltage-gated particle channels, which open just when the layer voltage is inside a specific range. Voltage clamp estimations of current are made conceivable by the close synchronous advanced subtraction of transient capacitive streams that go as the chronicle terminal and cell film are charged to modify the cell's potential.

Figure 2.1 shows the traditional voltage clamp method, which was invented by G. Marmant & K. Cole (Independently) in 1949 and used by Hodgkin & Huxley in 1952 [3].

Voltage Clamp Circuit Diagram

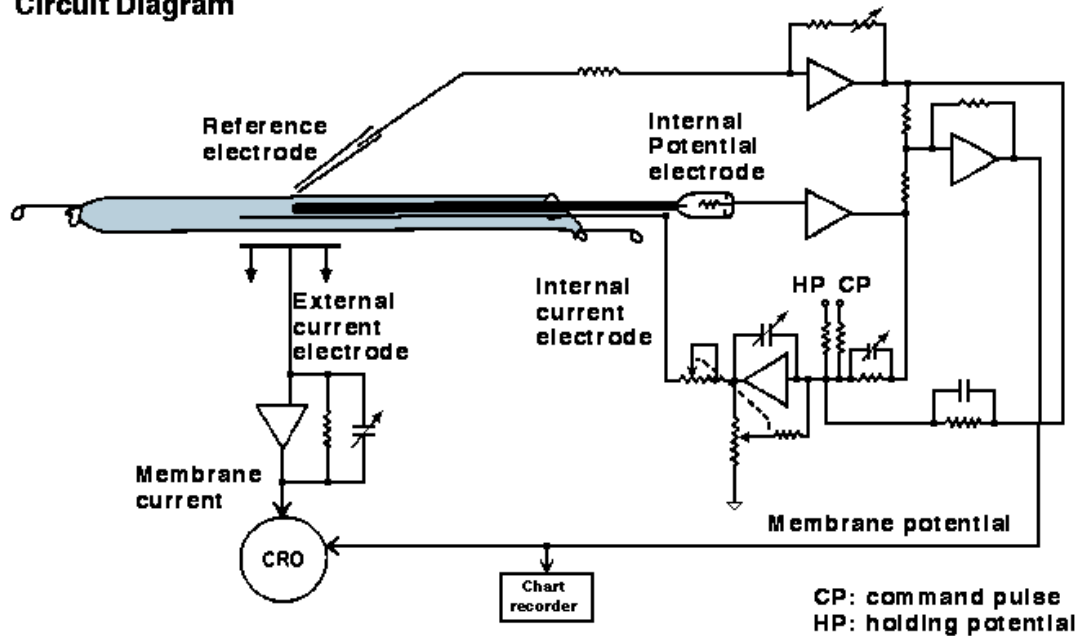


Figure 2 Voltage clamp used by Hodgkin & Huxley in 1952

Figure is adopted from Prof. Ying Sun*'s lab manual

*Biomedical engineering scientist and program director at the university of Rhode Island)

As the figure shows, the voltage clamp utilizes a negative input component. The layer potential intensifier measures film voltage and sends yield to the feedback amplifier. The feedback amplifier subtracts the layer voltage from the charge voltage, which it gets from the signal generator. This signal is enhanced and returned into the cell through the chronicle terminal, which is known to be the recording electrode. This methodology is still being used with the exception that a small axon needs to be used,

which cause major difficulty during experiments. The single electrode method of the Universal clamp solves this issue as it will be explained in detail in section 2.6.

2.3 Current Clamp

The current clamp method records the layer potential by infusing current into a cell through the account cathode. Not at all like in the voltage clamp method, where the film potential is held at a level dictated by the experimenter, in mode the layer potential is allowed to shift, and the enhancer records whatever voltage the cell produces without anyone else or because of incitement. This method is utilized to consider how a cell reacts when electric current enters a cell; this is imperative for example for seeing how neurons react to neurotransmitters that demonstration by opening layer particle channels.

Most current clamp amplifiers give practically no intensification of the voltage changes recorded from the phone. The amplifier is really an electrometer, once in a while alluded to as a "solidarity pick up enhancer"; its primary reason for existing is to diminish the electrical load on the little flags (in the mV go) delivered by cells with the goal that they can be precisely recorded by low-impedance hardware. The speaker builds the current behind the flag while diminishing the opposition over which that present passes. Consider this case in view of Ohm's law: A voltage of 10 mV is produced by passing 10 nanoamperes of current crosswise over 1 MOhm of obstruction.

2.4 Dynamic Clamp

Dynamic clamp uses a real-time interface between one or several living cells and a computer or analog device to simulate dynamic processes such as membrane or synaptic currents in living cells [4, 5].

2.5 Patch Clamp

The Patch clamp method was created by Erwin Neher and Bert Sakmann who got the Nobel Prize in 1991. Customary intracellular chronicle includes skewering a phone with a fine terminal; fix clip recording adopts an alternate strategy. A fix brace microelectrode is a micropipette with a generally substantial tip breadth. The microelectrode is put by a cell, and delicate suction is connected through the microelectrode to draw a bit of the cell layer into the microelectrode tip; the glass tip frames a high opposition 'seal' with the cell layer. This setup is the "cell-appended" mode, and it can be utilized for concentrate the action of the particle directs that are available in the fix of layer. On the off chance that more suction is currently connected, the little fix of film in the terminal tip can be uprooted, leaving the anode fixed to whatever remains of the cell. This "entire cell" mode permits exceptionally stable intracellular account. A detriment (contrasted with traditional intracellular account with sharp terminals) is that the intracellular liquid of the cell blends with the arrangement inside the chronicle anode, thus some imperative segments of the intracellular liquid can be weakened. A variation of this system endeavors to limit these issues. Refer to the figure to see a sample of the patch clamp 4 different methods of measuring.

Patch Clamp Configurations

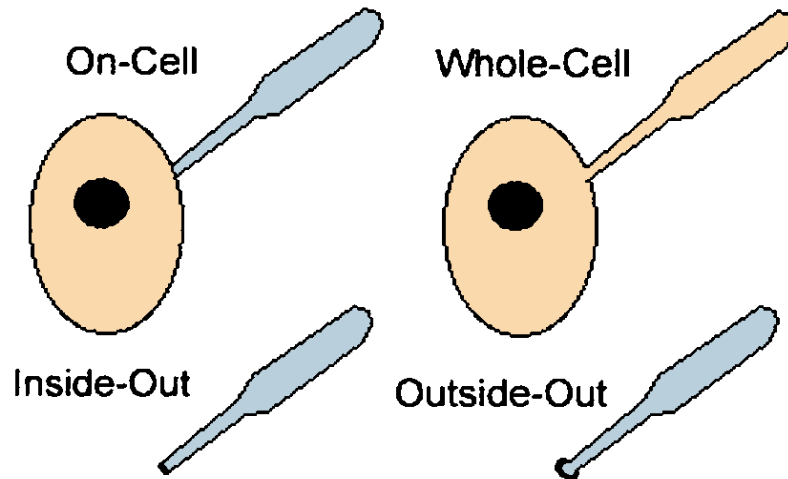


Figure 3 Patch clamp configurations

2.6 Universal Clamp

The universal clamp has a faster loop which is not limited by PC ability. It also uses a standard software, hardware is standard as well for control, windows which is not optimized for operation. Therefore, it is more insufficient. It was more customized, monitoring and data acquisition only, the front end implements the control; while the old system has only one end. The new system has both which separate and minimize cost, easier to repair, and it has smaller customized processors.

2.7 List of References

1. Sun Y, Wu J, Collis L, Hill RB. Apparatus for neuromuscular measurement and control. Patent no. US 7,489,965 B2, February 10, 2009.
2. Sun Y, Wu J, DiCecco J, Hill RB. Processor controlled voltage-current analysis of nerve and muscle tissues. Patent no. US 8,000,783 B2, August 16, 2011.

3. Hodgkin & Huxley, (1952). 'Currents carried by sodium and potassium ions through the membrane of the giant axon of Loligo.' *Journal of Physiology*, 116, 449-472.
4. Sharp AA, O'Neil MB, Abbott LF, Marder E (1993a) Dynamic Clamp: Computer-Generated Conductances in Real Neurons. *J Neurophysiol.* 69:992-995.
5. Sharp AA, O'Neil MB, Abbott LF, Marder E (1993b) The dynamic clamp: artificial conductances in biological neurons. *Trends Neurosci.* 16:389-394

CHAPTER 3

NEURON EMULATOR

3.1 Introduction

The Neuron Emulator (NE) plays an important role in this thesis research for testing the various functions of the Universal Clamp. In this chapter, the NE previously developed in the URI Biomedical Engineering Lab is first reviewed. The specific contributions of this thesis to the instrumentation of the NE include the construction of the latest version of the NE on a breadboard and the attempts to improve the NE regarding its rise time (section 3.5).

The NE is intended to represent both the passive electrical properties and the active electrical properties of a live neuron. The passive property is mainly the resistance and capacitance of the cell membrane of the neuron. The active property of the neuron pertains to the firing of the action potentials. In 2004-2005 [1, 2], the first-generation NE was developed, which produced a voltage waveform of the action potential. The NE had a current input port and a voltage output port. In response to the input current (stimulation) the NE was able to adjust the firing rate of the action potentials accordingly. While the first-generation NE was able to present action potentials for the purposes of teaching and testing the neuroscience instruments, it could not be voltage clamp. The first-generation NE was based on a voltage source, which always produced a sufficient current to maintain the wave shape of the action potential and could not be cancelled out by an external feedback current.

Thus, in 2011 the development of the 2nd-generation NE was started with the intention that the NE is responsive to voltage clamping [3]. The circuit design was completed redone and centered around the concept of a capacitance source. Instead of using a voltage source or a current source, a capacitor is pre-charged and switched on at appropriate times to produce the action potential. Because the charge on the capacitor is limited, the action potential can be clamped by use of an external feedback current to cancel out the discharge of the capacitor. The design was novel and resulted in a US patent [4].

3.2 Neuron Emulator Innovation

The patent illustrated the following, ‘this invention was concerned with an electronic neuron emulator for a single-electrode setting that has both the passive properties (membrane resistance and capacitance) and the active properties (action potential) of a live neuron. A unique design feature is that the currents used to generate action potentials come from a pre-charged capacitor. Unlike a voltage source or a current source, the charge on the capacitor is limited, thereby providing a more realistic condition for testing neuroscience instruments such as the single-electrode voltage clamp and the patch clamp.

Currently the standard device for testing electronic neuroscience instruments such as a voltage clamp amplifier is a simple resistor-capacitor (RC) circuit. While the RC circuit can represent the passive electrical properties of a live neuron, it cannot generate action potentials to interact with the voltage clamp amplifier in a dynamic way.

Previously we developed a neuron emulator that used an oscillator to generate the action potentials [1]. The oscillator was a time-varying voltage source, which was too strong to overcome by use of a voltage clamp amplifier. Thus, it was not possible to voltage-clamp the action potentials generated by our previous device. The neuron emulator in this invention is based on a totally different concept. An action potential is generated by switching a pre-charged capacitor into the output circuitry. Once the capacitor is discharged, it is switched out of the output circuitry and charged up for the next firing of the action potential. A microprocessor is embedded in the device to provide controls of the firing of the action potentials. This concept was first published in [2] on April 3, 2011.

3.3 Theory of Operation of the Neuro Emulator

The patent illustrated the following, ‘this invention was concerned with an

Figure 3.2.1 contains the circuit diagram of the neuron emulator, a typical patch clamp setting that the circuit attempts to emulate, and the switching signals and the resulting action potential output. The passive properties of the neuron are represented by the circuit of R_m in parallel with C_m , which is connected to a voltage reference representing the resting membrane potential V_{rest} . The active properties of the neuron are represented by the circuit of R_{ap} in parallel with C_{ap} , which is intermittently connected to V_{peak} for pre-charging. To fire an action potential, the R_{ap} - C_{ap} circuit is switched in series with the R_m - C_m circuit. After discharging, the R_{ap} - C_{ap} circuit is switched out, leaving the R_m - C_m circuit connected to the resting membrane potential V_{rest} . The switching operation is accomplished by three switches S_1 , S_2 , and S_3 . These switches are controlled by a microprocessor. The output of the R_m - C_m circuit

represents the membrane potential of the neuron and is sent to the analog-to-digital converter via an amplifier. Thus, the microprocessor can constantly monitor the membrane potential and adjust the firing rate accordingly. The output of the Rm-Cm circuit can also be accessed externally via resistor R_a as the output voltage V_{out} , where R_a represents the resistance of the electrode. The timing of the switching signals is done in such a way that the action potential is generated by turning S1 and S2 off and S3 on.

The figure further describes the switching of the Rap-Cap circuit in two stages. Stage 1 represents the resting potential as S1 and S2 are on and S3 off. The Rap-Cap circuit is disconnected from the Rm-Cm circuit and is charged by V_{peak} . Stage 2 represents the action potential as S1 and S2 are off and S3 on. The Rap-Cap circuit is connected in series with the Rm-Cm circuit. The output V_{out} momentarily jumps to V_{peak} and then discharges. The firing of consecutive action potentials is accomplished by alternating between stage 1 and stage 2.

The aforementioned neuron emulator produces an action potential that has the waveform of a simple exponential discharge. This waveform can be further improved and made closer to a real action potential. Figure 3.2.3 shows a more sophisticated design using two RC circuits in parallel to generate the action potential. Furthermore, the circuit elements are tuned to bear physiological relevance. The example shown in Fig. 3.2.3 represents the squid giant axon with parameters from the work of Hodge and Huxley. In this model the RNa-CNa circuit represents the sodium channel, and the RK-CK circuit represents the potassium channel. Many other variations are possible

by tuning the circuit parameters and/or adding additional R-C circuits to represent different ionic channels for the generation of action potentials.

The neuron emulator was successfully built and tested. Figure shows the switching signal, the computer-simulated action potential and the action potential generated by the neuron emulator. Figure shows the result of a step clamp experiment with the neuron emulator, in which the firing rate of the action potential increased as the membrane potential raised by the externally injected current.

The figure is an annotated screenshot of an oscilloscope during a voltage clamp experiment. A commercial voltage clamp amplifier was connected to the neuron emulator and successfully implemented a voltage clamp. An action potential was generated at each on-set of the switching signal shown on channel 3 (CH3). The output voltage was successfully clamped to a constant voltage as shown on channel 2 (CH2). The feedback current responsible for canceling out the action potential was shown on channel 1 (CH1) [3].

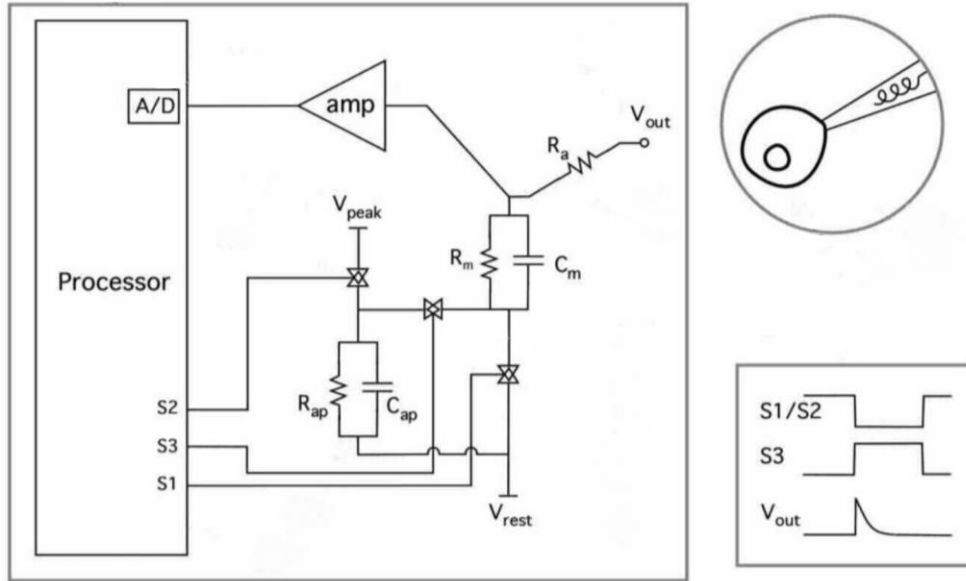


Figure 4 The circuit diagram of the neuron emulator

Stage 1. Resting Potential
(S1 & S2 on; S3 off)

Stage 2. Action Potential
(S1 & S2 off; S3 on)

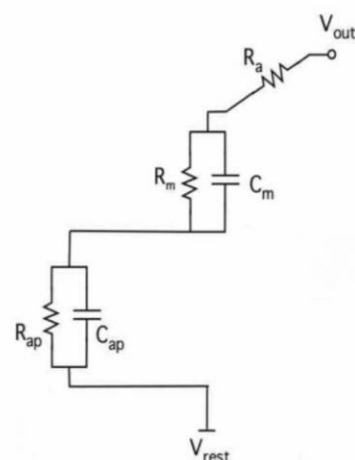
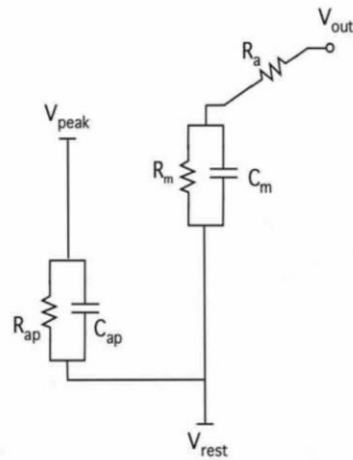


Figure 5 The switching of the Rap-Cap circuit in two stages

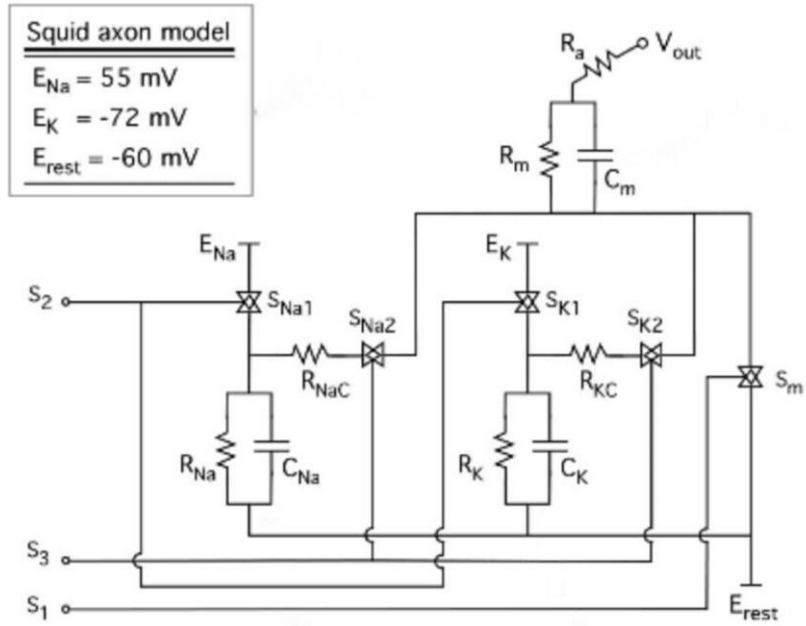


Figure 6 The squid giant axon with parameters from the work of Hodge and Huxley

3.4 Preliminary Testing Results

The preliminary testing results are summarized here.

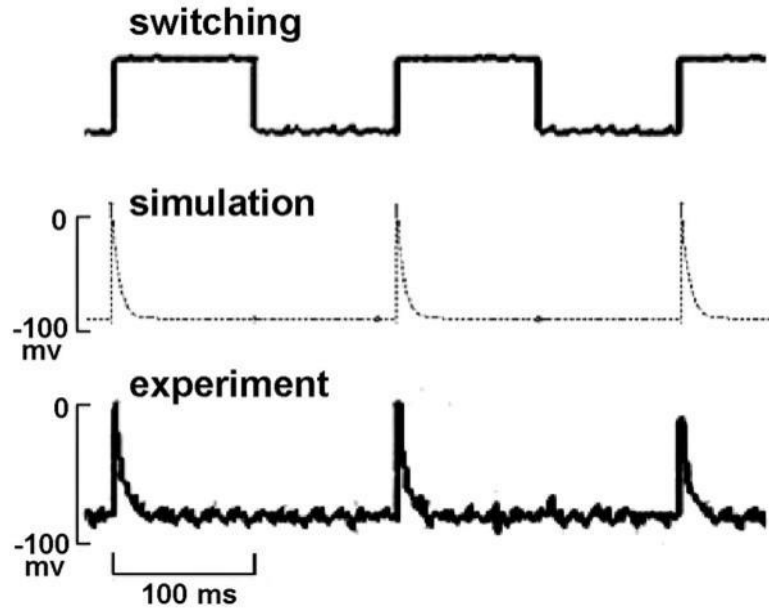


Figure 7 Shows the switching signal

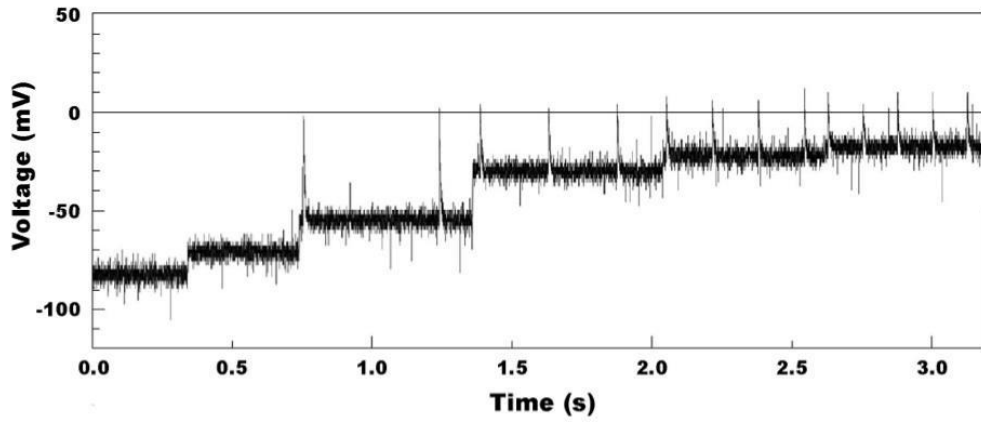


Figure 8 The result of a step clamp experiment with the neuron emulator

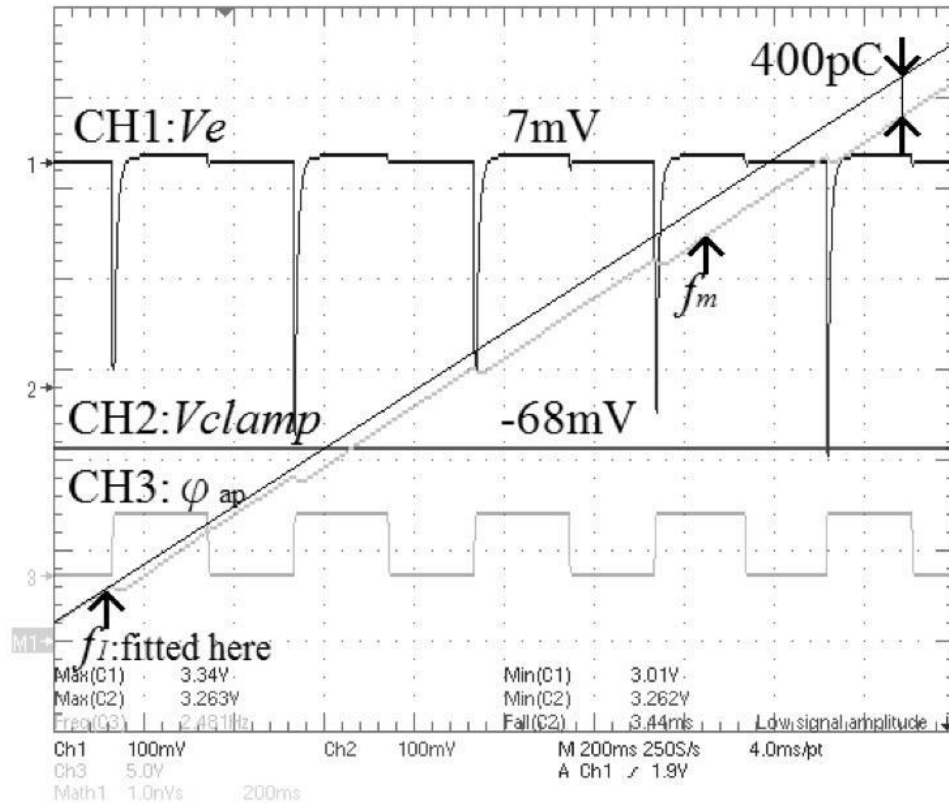


Figure 9 Waveforms of the NE output (CH1), voltage clamped result (CH2) and switching signal (CH3)t

3.5 Attempt to Increase the Rise Time

While the second-generation NE represents both the passive electrical properties and the active electrical properties of the neuron and is responsive to voltage clamp, it does have a drawback associated with a fast rise time. The rise time of an action potential is defined by the time to rise from 10% to 90% of the peak magnitude. The typical rise time for an action potential of a biological neuron is on the order of 1 ms [5]. The rise time for the NE is on the order of 0.01 ms, about 100 times faster. This is because the switching of the pre-charged capacitor into circuit results in an almost instantaneous change of the output voltage. While the fast rise time challenges the voltage clamp amplifier to be tested.

3.5.1 Attempt to Increase the Switching Time

The first attempt to increase the rise time is by slowing down the switching process. The switching is accomplished by use of an analog switch integrated circuit LM14016 [6]. During the on stage, this analog switch has a resistance of about 250 ohms. During the off stage, the leakage current is about 50 pA. However, the datasheet does not specify the timing related parameters. It is hypothesized that by increasing the rise time of the control signal, the transition time of the output channel resistance increases accordingly. Thus, an experiment was conducted according to the instrumentation in the figure, panel A. A MC14016 IC chip was powered by a 5V portable charger. A function generator is used to produce a waveform with an amplitude between 0 and 5V. The control waveform is displayed on channel 1 (CH1) an oscilloscope. The output switch connects the 5V supply to channel 2 (CH2) of the oscilloscope.

The function generator produced three different waveforms (square wave, triangular wave, and sinusoidal wave) as shown in Figure 3.5.1, panel B, C, and D, respectively. The resulting output switching waveforms indicated that the rise time was not affected. Thus, the hypothesis of reducing the output switching time by reducing the rise time the switch control signal was invalidated.

The result suggested that the MC14016 analog switch circuit likely employs a Schmitt trigger circuit that activates at a threshold voltage of above 2.5 V, or half of the supply voltage. Once the input control signal reaches the threshold, the output analog switch is turned on instantaneously. As shown in Figure 3.5.1, panel B, the square wave input resulted in an immediate switch of the output. As shown in Figure

3.5.1, panel C, the triangular wave input resulted in a delay; the output switched instantaneously when the input reached 2.5 V. As shown in Figure 3.5.1, panel D, the sinusoidal wave input resulted in a delay; the output also switched instantaneously when the input reached 2.5 V.

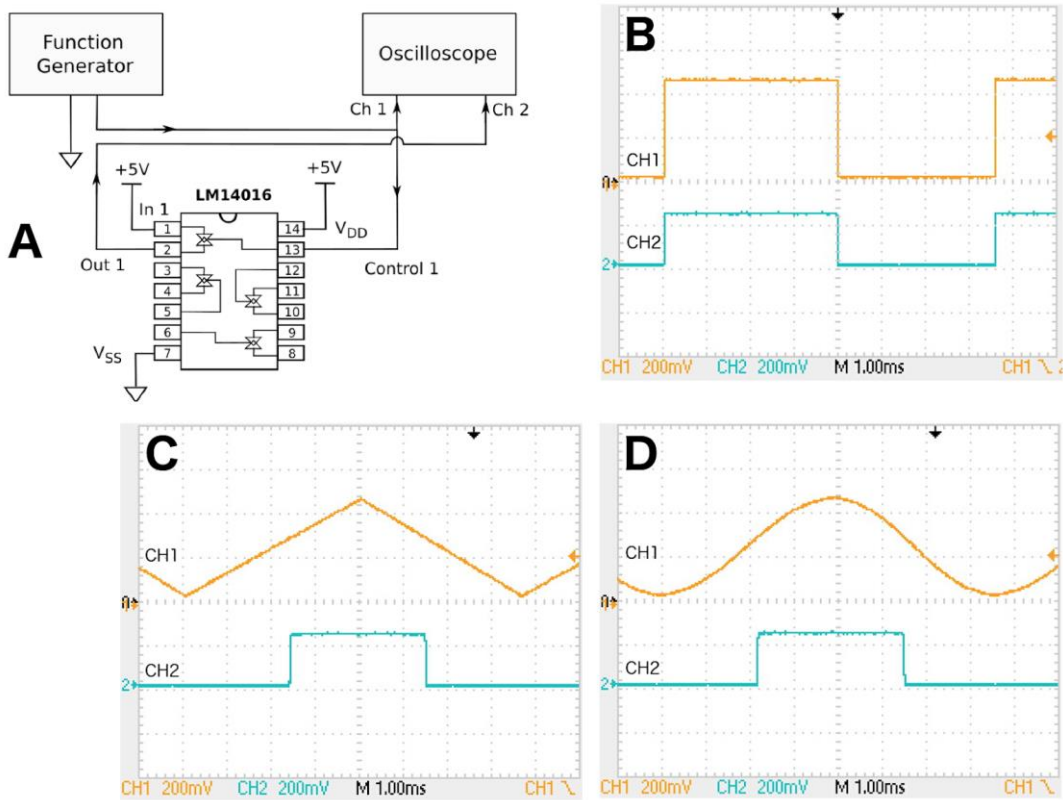


Figure 10 Panel A: Instrumentation for testing the rise time of the analog switch (MC14016). Panel B: Result of using a square wave input. Panel C: Result of using a triangular wave input. Panel D: Result of using a sinusoidal wave input

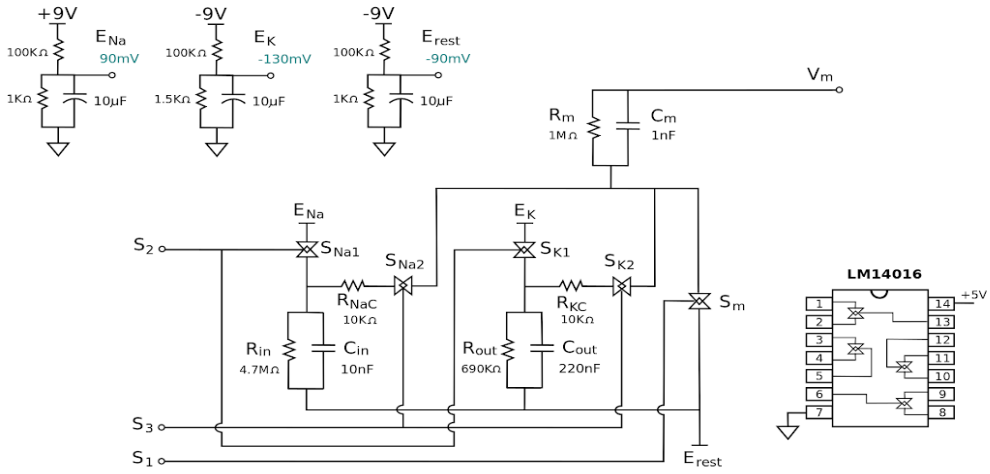
3.5.2 Adding a Low-Pass Filter at the Output

The second attempt to increase the rise time is by adding a low-pass filter at the output of the NE. The original schematic diagram of the NE is shown in Figure 3.5.2, panel A. The action potential is generated by switching the sodium (Na) channel and the potassium (K) channel in series with the membrane $R_m C_m$ circuit.

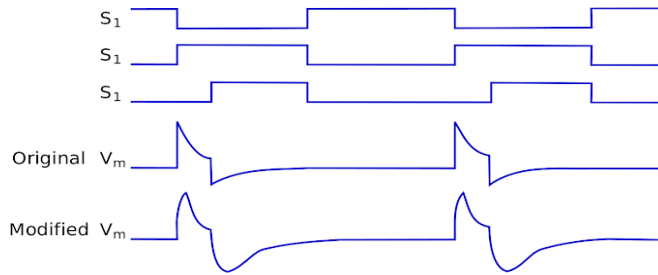
Each channel is represented by an RC circuit with the capacitor pre-charged to a specific voltage. To fire the action potential, the voltage source that charges the capacitor is disconnected and the capacitor is switched in series with the membrane $R_m C_m$ circuit. The Na channel is switched in first to cause the initial depolarization of the action potential. The potassium channel is switched in later to cause the repolarization and hyperpolarization of the action potential. The waveforms of the switching signals (S_1 , S_2 , and S_3) and the resulting action potential are shown in the figure, panel B. The modified schematic diagram of the NE is shown in the figure, panel C. A low-pass filter (R_f and C_f) is added to the output circuit with the intention to slow down the surge as shown by the highlighted parts of the modified NE circuit. The time constant is: $R_f \times C_f = 1 \text{ M}\Omega \times 1 \text{ nF} = 1 \text{ ms}$, which is the typical rise time for the action potential of a biological neuron.

The NE has been implemented on a breadboard by using a 18F525 processor (Microchip, Chandler, AZ) as the controller, as shown in Figure 3.5.3.

A. Original Schematic Diagram



B. Switching Signals



C. Modified Schematic Diagram

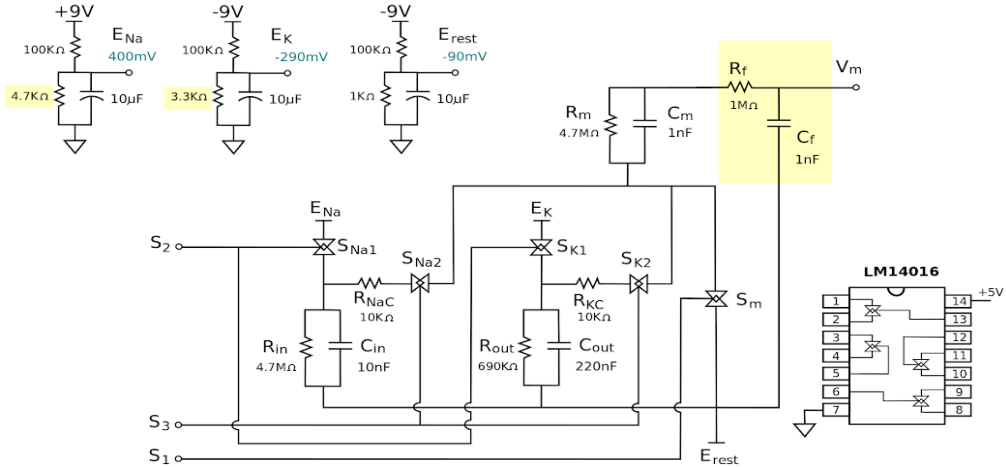


Figure 11 Panel A: Original schematic diagram of the 2nd-generation NE. Panel B: Waveforms for the switching signals, Panel C: Modified schematic diagram by adding a low-pass filter at the output

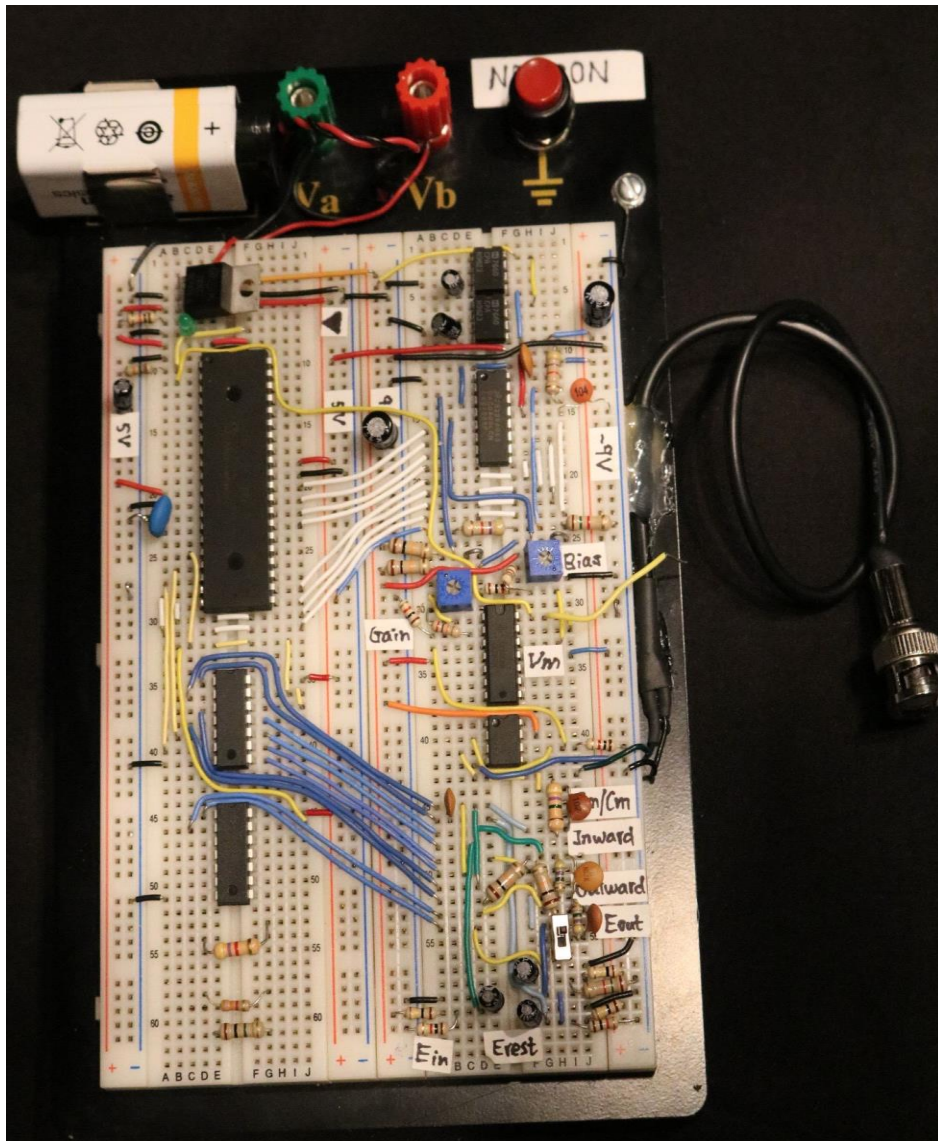


Figure 12 The Neuron Emulator (NE) implemented on a breadboard

Figure shows the action potentials generated by the original NE (panels A-C) and the action potentials generated by the modified NE with the output low-pass filter (panels D-F) at different time resolutions. From panel C, the rise time for the action

potential of the original NE is about $15 \mu\text{s}$. From panel F, the rise time for the action potential of the modified NE is about $700 \mu\text{s}$.

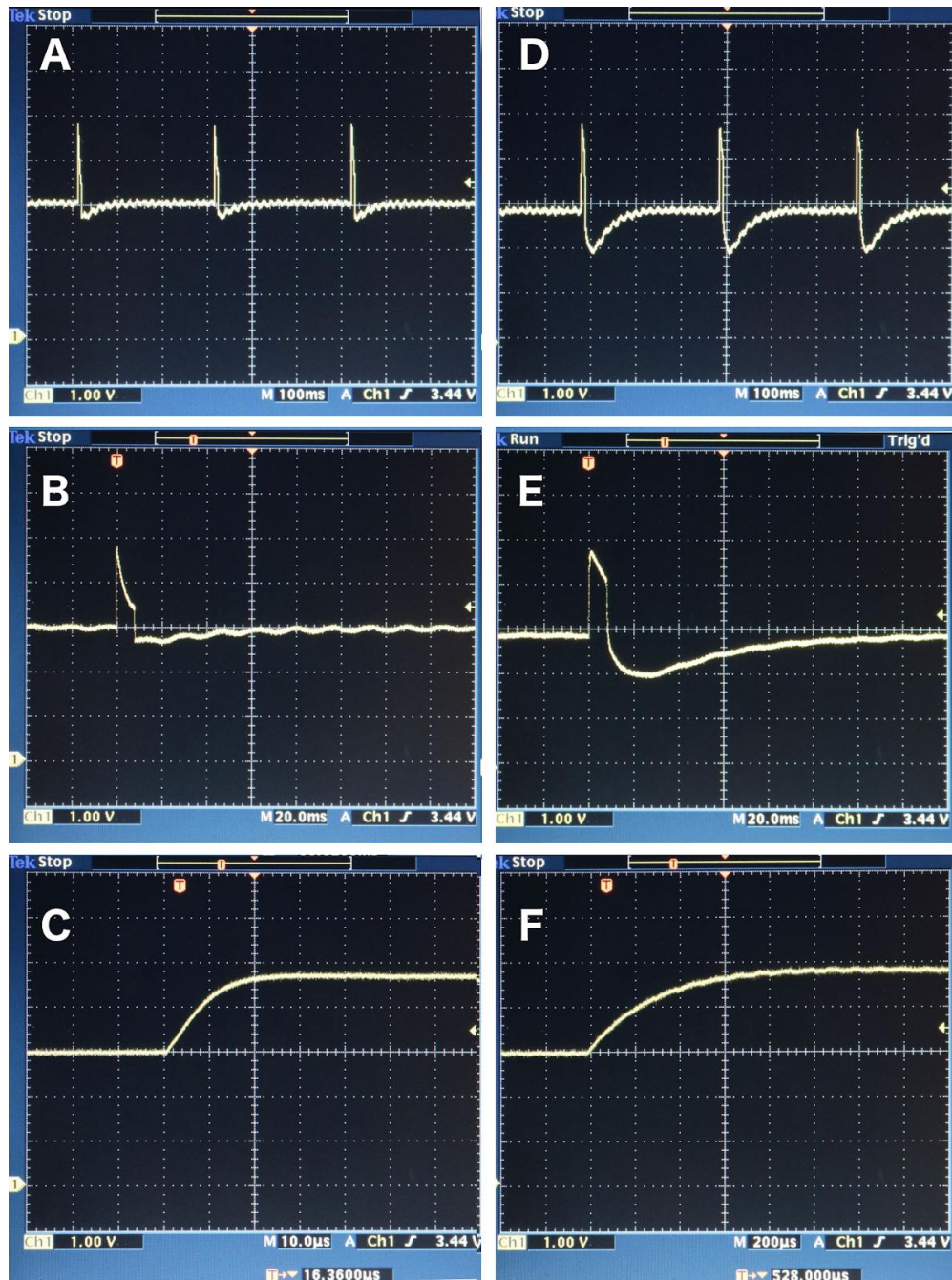


Figure 13 Action potentials generated by the original NE are shown on the left (panels A-C) at different time resolutions. Action potentials generated by the modified NE with the output low-pass filter are shown on the right (panels D-F) at different time resolute

In summary, adding a low-pass filter can shape the action potential of the NE with a rise time comparable to that of the biological neuron. However, the added capacitance also limits the response of the feedback loop during voltage clamp. As

discussed in more detail in Chapter 5, the modified NE does not help to improve the voltage clamp performance.

3.6 List of references

1. Wu J, DiCecco J, Sun Y, Hill R. An analog neuron emulator for education and testing of neurophysiological instruments. Society for Neuroscience 34th Annual Meeting, San Diego, CA, October 23-27, 2004.
2. Breau F, Maio-Cannon S, Davis R, Wu J, DiCecco J, Sun Y. The neuron emulator: an undergraduate biomedical engineering design project. 31st Annual Northeast Bioengineering Conference, Hoboken, NJ, pp. 29-30, April 1-3, 2005.
3. Wu YC, Chen JY, Rieger R, Sun Y. A neuron emulator for single-electrode settings. 37th Annual Northeast Bioengineering Conference, Rensselaer Polytechnic Institute, Troy, NY, April 1-3, 2011.
4. Sun Y, Rieger R. Apparatus for memristor/neuron emulation and testing. U.S. Patent 8,990,137 B2 issued Mar. 24, 2015.
5. Purves D, Augustine GJ, Fitzpatrick D, Katz LC, Anthony-Samuel LaMantia AS, McNamara JO, and S Mark Williams SK (editors). Neuroscience. Sunderland (MA): Sinauer Associates, ISBN-10: 0-87893-742-0, 2001.
6. Semiconductor Components Industries, LLC. MC14066B Quad Analog Switch/Quad Multiplexer (Rev. 3). On Semiconductor, <http://onsemi.com>, March, 2000.

CHAPTER 4

CELL CAPACITANCE EMULATOR

4.1 Background

The cell membrane consists of the lipid bilayer that has a fairly constant specific capacitance ($0.9 \mu\text{F}/\text{cm}^2$). Thus, the cell capacitance is generally proportional to the cell surface area. Monitoring the cell capacitance can reveal changes of the cell surface area. Exocytosis is the secretion process that the cell directs the contents of a vesicle to the extracellular space. Conversely, endocytosis is the process that the cell takes in substances from outside via vesicle formation and transport. The mergence of a vesicle into the cell membrane momentarily increases the cell surface area, thereby changing the cell capacitance. The whole cell capacitance is typically 3-12 pF. The capacitance signal from a single vesicle is typically 1-15 fF, about 1/1000 of the whole cell capacitance. The duration of a vesicle crossing the cell membrane is about 2 ms. To measure a small capacitance, change on the order of 10 fF with a duration on the order of 1 ms is very challenge but possible.

4.2 Introduction to the Cell Capacitance Emulator

The cell capacitance emulator (CCE) is a simulation tool for testing a neuroscience instrumentation system that measures (or attempts to measure) the dynamic changes of the cell membrane capacitance of a neuron. The CCE circumvents the use of live cells in the instrumentation testing, which generally requires a high level of experimental skills in electrophysiology and could be very time-consuming to set up. While the CCE does not replace a live neuron in many respects, it

provides a gold standard on the capacitance change and a consistent measurand for the instrument to be tested.

Like the Neuron Emulator, the CCE also plays an important role in this thesis research for testing the capacitance measurement capability of the Universal Clamp. A prototype of the CCE was developed in the URI Biomedical Engineering Lab in 2016. The specific contribution of this thesis is to construct a CCE on a breadboard and to improve its functionality.

4.3 Instrumentation of the Cell Capacitance Emulator

The smallest capacitance value for the standard capacitors available from the electronic suppliers is 4.7 pF, which is about 3 orders of magnitude larger than that of the vesicle capacitance (~ 10 fF). The idea behind the cell capacitance emulator is to represent the dynamics of the vesicle capacitance by switching between two circuit branches that have a small difference in the capacitance values. For example, if the total cell capacitance is represented by 10 pF, two capacitors can be chosen such that one has 10.00 pF and the other 10.01 pF. By switching between the two capacitors, the difference of 0.01 pF (or 10 fF) can represent the small capacitance change due to a vesicle crossing the cell membrane.

A capacitance meter with the highest precision (Model 3000, GLK Instruments, San Diego, CA) is capable of measuring capacitance down to the precision of 1 fF [2]. The schematic diagram of the CCE and the instrumentation setup with the Universal Clamp and the capacitance meter are shown in Figure 4.3.1.

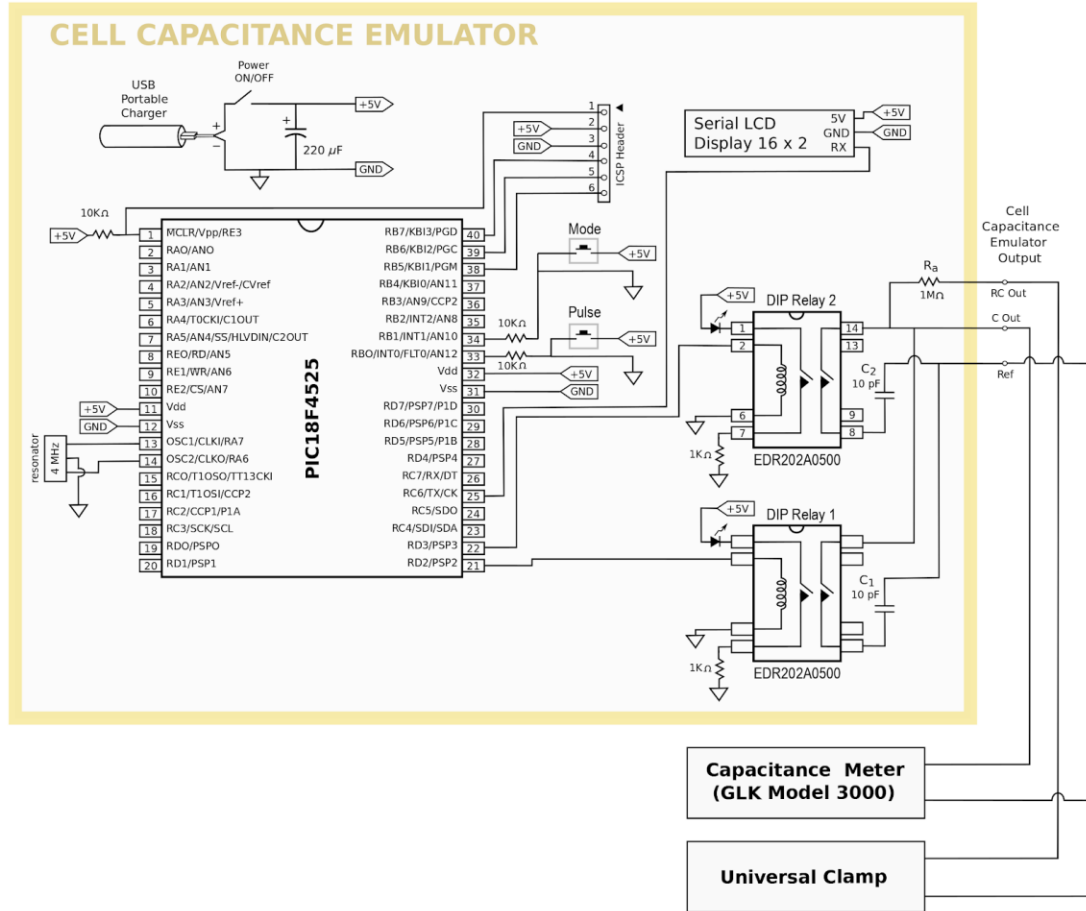


Figure 14 The schematic diagram of the CCE and the instrumentation setup with the Universal Clamp and the capacitance meter

The CCE outputs a dynamic RC circuit. The resistor R_a ($1\text{ M}\Omega$) represents the cell membrane resistance. The capacitor presenting the cell membrane capacitance is switched between C_1 and C_2 . Both capacitors are 10 pF ; however, they are chosen such that there is a small difference between them. The differential capacitance represents the vesicle capacitance. This dynamic RC circuit is used as the input to the Universal Clamp. The purpose of the Universal Clamp is to detect the vesicle activities as discrete events, not to measure the exact value of the vesicle capacitance.

The CCE also has a capacitance-only output, which is sent to a precision capacitance meter for determining the exact capacitance values of C_1 and C_2 .

The switching between the capacitors (C_1 and C_2) is accomplished with two single-pole-double-throw relays. Originally, the analog switch IC (MC14016) used in the Neuron Emulator was intended to be employed here as well. However, the analog switch itself has a significant amount of capacitance. Thus, a mechanical switch needs to be used to minimize the contact capacitance. The mechanical relay switch has the disadvantage of a slow switching time as compared to the semiconductor analog switch. The final choice was the DIP reed relay EDR202A0500 [3], which has an operate time (closing) of 1 mS and a release time (opening) of 0.5 mS.

The CCE is controlled by a microprocessor (PIC18F4525, Microchip, Chandler, AZ). Two push buttons (Mode and Pulse) are used as the user interface. The Pulse button is used to activate the output by engaging the two relays. Two of the I/O outputs (RD2 and RD3) are used to control the two relays. During the output phase, RD2 and RD3 are always opposite to allow only one capacitor (either C_1 or C_2) connected to the output circuit Y. When the Pulse button is pushed, the CCE sends out a burst of 10 vesicle capacitance pulses and then stops. The pulse repetition rate is 1 Hz. A total of 7 operational modes are available as shown in Table. The Mode button allows the user to select the operating mode. The pulse width can be set to 500 ms, 200 ms, 50 ms, 10 ms or 2 ms (Modes 1-5). Modes 6 and 7 are used to present a constant capacitance output to the precision capacitance meter, which determines the precise value of C_1 or C_2 . An LCD character display (16 characters x 2 rows) is used to show the selected mode.

Table 1 Operation modes for the Cell Capacitance Emulator

Mode	Pulse Repetition Rate	Relay 1 (controlled by RD2)	Relay 2 (controlled by RD3)
1	1 Hz	On 500 ms, Off 500 ms	Off 500 ms, On 500 ms
2	1 Hz	On 200 ms, Off 800 ms	Off 800 ms, On 200 ms
3	1 Hz	On 50 ms, Off 950 ms	Off 950 ms, On 50 ms
4	1 Hz	On 10 ms, Off 990 ms	Off 990 ms, On 10 ms
5	1 Hz	On 2 ms, Off 998 ms	Off 998 ms, On 2 ms
6	N/A	On always	Off always
7	N/A	Off always	On always

The CCE has been implemented on a breadboard as shown in Figure 4.3.2. It is powered by a portable USB charger that outputs 5V. The firmware has been developed in the C++ language by use of MPLab X (Microchip, CHandler, AZ) and programmed via a PICKit 3 in-circuit development module.

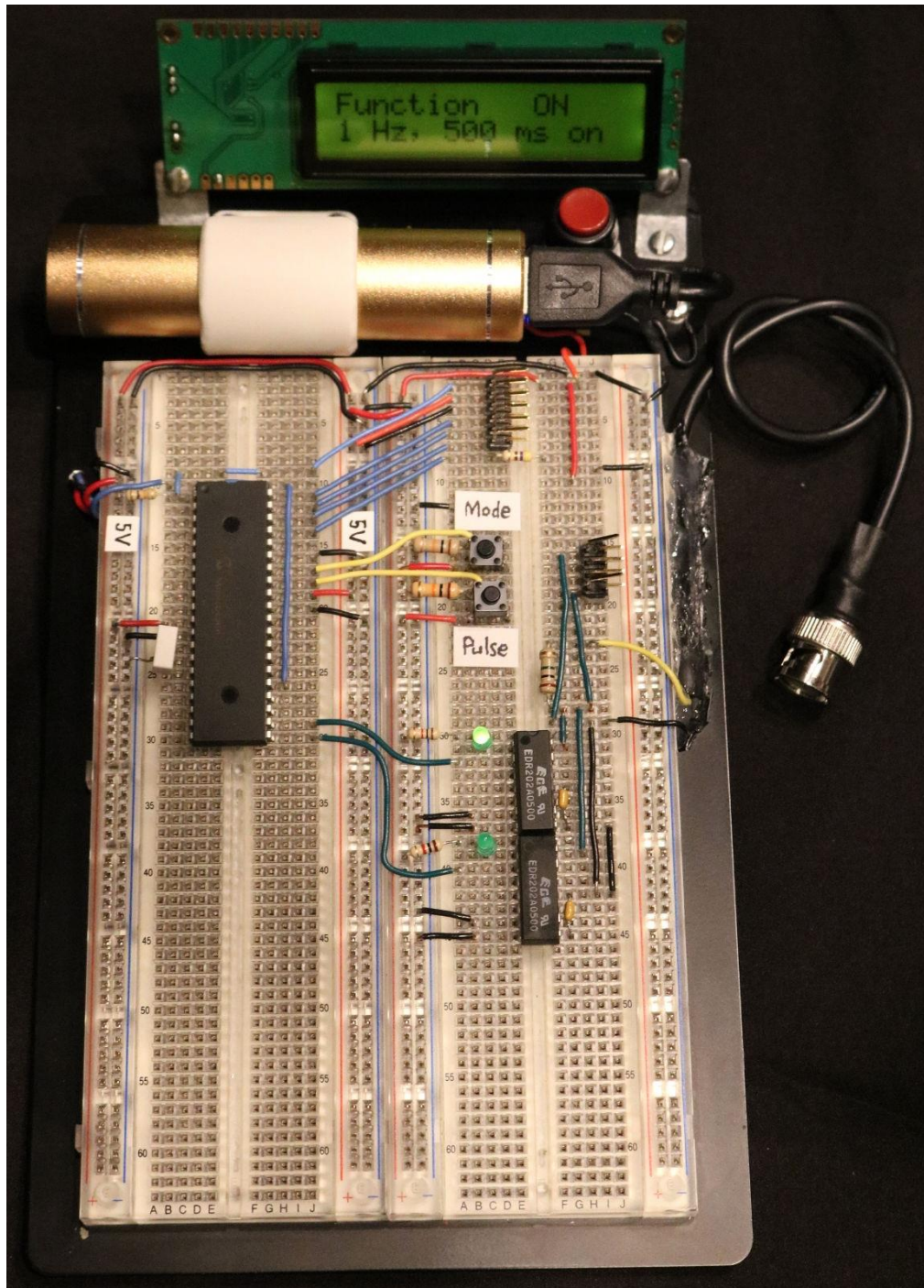


Figure 15 The Cell Capacitance Emulator (CCE) implemented on a breadboard
 4.4 List of References

1. Rosenberg L, Hammick M, Sladen S, Wang T, Wu J, & Sun Y. An Electronic Model for Vesicle Induced Cell Membrane Capacitance Changes. 42nd Ann

Northeast Bioengineering Conference, SUNY Binghamton, Vestal, NY, April 5-7, 2016.

2. GLK Instruments. Model 3000 Digital Capacitance Meter: Operation and Calibration Manual, version 3.3. <http://www.glkinst.com/cmtrdocs/Instruction%20and%20Service%20Manual_revision_3.3.pdf>. Retrieved in October 2017.
3. Excel Cell Electronic Co., Taiwan. EDR202A0500 DIP Reed Relay Datasheet. <<https://www.digikey.com/products/en?keywords=edr202>>. Retrieved in October 2017.

CHAPTER 5

METHODS FOR MEASURING CELL CAPACITANCES

5.1 Introduction

The Nobel Prize in Physiology or Medicine 2013 was awarded jointly to James E. Rothman, Randy W. Schekman and Thomas C. Südhof "for their discoveries of machinery regulating vesicle traffic, a major transport system in our cells" [1]. The previous studies on the vesicle activities have been mainly based on electron microscopic imagery of nonliving cells. The possibility of monitoring the vesicle activities by measuring the cell capacitance changes in live cells presents a groundbreaking technology in obtaining a much better insight into the cellular physiology and pharmacology. As mentioned in Chapter 3, the cell capacitance change due to a vesicle crossing the cell membrane is about 10 fF with a time interval of 2 ms. Measuring this vesicle-induced capacitance change is possible but very challenging.

5.2 Existing Method

Recent studies have shown the possibility of measuring this capacitance signal. For example, Rituper et al. [2] demonstrated a method for high-resolution membrane capacitance measurements. A system based on a lock-in amplifier was able to measure the admittance of the cell, consisting of a real part (conductance) and an imaginary part (susceptance). As shown in the Figure 5.2.1(from Rituper et al.), changes of the susceptance related to vesicle discharges were observed.

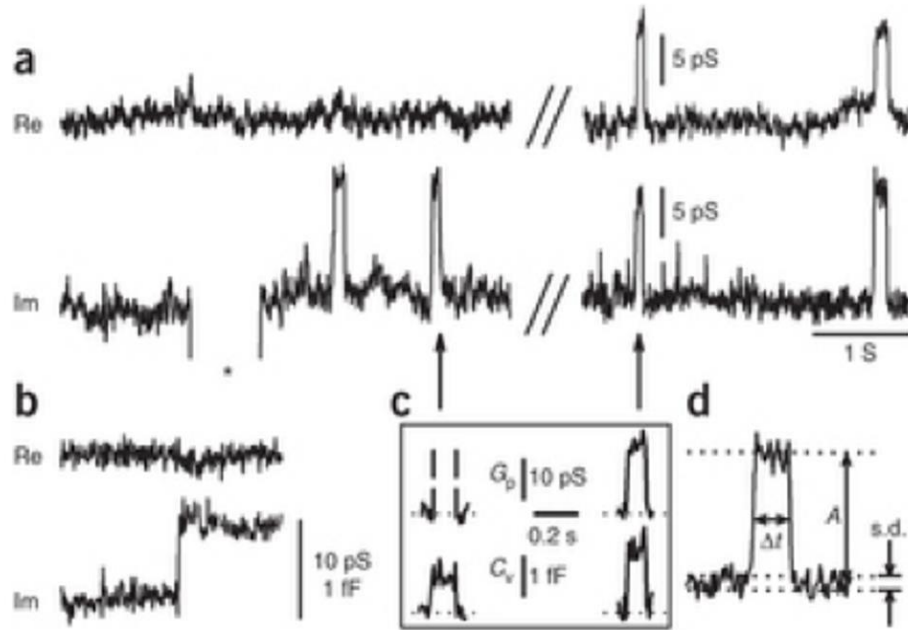


Figure 16 High-resolution membrane capacitance measurements for the study of exocytosis and endocytosis, adapted from Rituper et al. [2]

The instrumentation system was rather complicated that required multiple instruments including a patch-clamp amplifier and a lock-in amplifier. Signal processing techniques such as signal averaging were used to improve the signal-to-noise ratio. The requirements of post (off-line) processing make this method difficult for real-time applications.

5.3 A Frequency-Domain Method

The current version of the Universal Clamp has a preliminary vesicle detection algorithm, which was implemented by Dr. Jiang Wu. The algorithm was based on the short-time Fourier transform [3] as described below.

The standard Sampling rate in the Universal Clamp is 20 MHz. For vesicle detection, the sample points are decimated by a factor of 20, which results in sampling rate of 1 MHz. A non-overlapping sliding window slides over the data stream. For each window, the fast Fourier transform (FFT) [4] is performed. The buffer length of

the FFT is 2048. Thus, the time resolution for the capacitance measurement is 488 Hz (1000000/2048). The current port of the Universal Clamp outputs a sinusoidal waveform of 488 Hz with a amplitude of 10 nA to excite the measurand.

The data are transferred from the front-end digital signal processor for the host PC laptop via an Ethernet link. Each packet contains 250 measurements. Thus, on the PC laptop end, the measurements come in every 0.512 s, which is barely sufficient to display the vesicle pulses of a 0.2s pulse width. The results are displayed as the magnitude and the phase of the short-time Fourier transform.

5.4 A Time-Domain Method

An innovative algorithm has been proposed to perform the vesicle capacitance detection by taking advantage of the Universal Clamp hardware and by optimizing the signal processing tactics [5]. The concept of the lock-in amplifier (using sinusoidal modulation and demodulation) is integrated into the detection algorithm. The Universal Clamp delivers a sinusoidal current excitation and performs a matched filter on the induced voltage, which has the same noise-reduction effect of an lock-in amplifier but without actually using one. The intended input and output waveforms are shown in Figure 5.4.1.

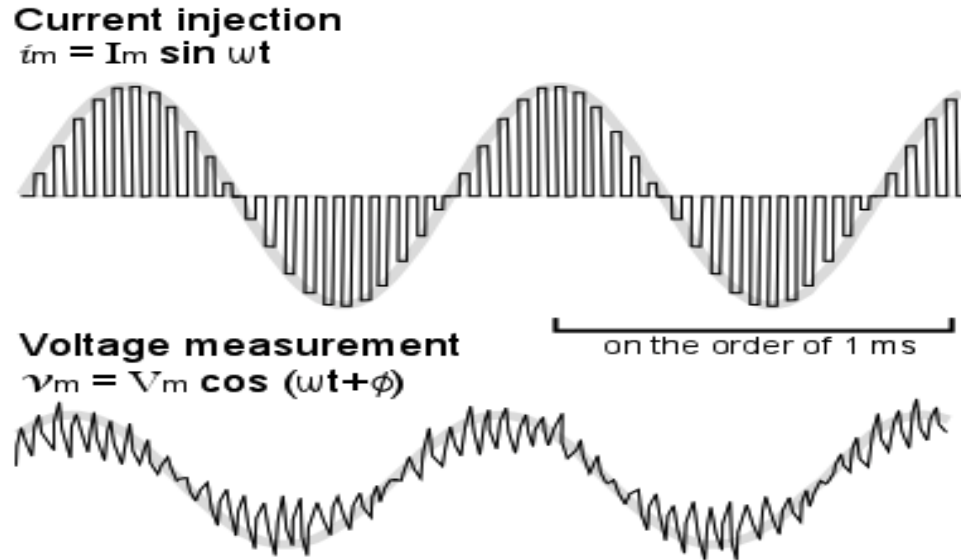


Figure 17 illustrates the concept of a switching excitation with sinusoidally amplitude-modulated current injection and an induced voltage that has a sinusoidal envelope with a phase shift

As shown in Figure 5.4.2, the measurand is modeled by a 3-element circuit with the access resistance R_a , and the cell membrane resistance R_m in parallel with the cell membrane capacitance C_m .

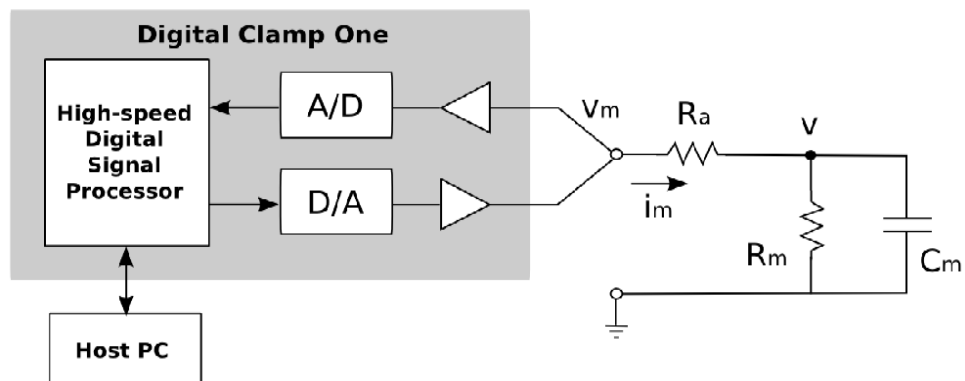


Figure 18 an illustrative diagrammatic view of the system that measures electrical properties of a measurand by time-multiplexing the current injection and the voltage measurement via a single port. The measurand is modeled as a 3-element circuit with a resistor

Representing the current (i_m) and voltage (v_m) with sinusoidal functions has the advantage that their derivatives have closed-form solutions. Thus, the circuit equations shown below can be directly fitted to a time-domain least-squares estimator as summarized below.

$$v_m' - R_a i_m' = \left(\frac{1}{C_m} + \frac{R_a}{R_m C_m} \right) i_m - \frac{1}{R_m C_m} v_m$$

Take N sample points over a full time period $2\pi/\omega$.

$$\begin{bmatrix} x_1 \\ x_2 \\ \dots \\ x_N \end{bmatrix} = \begin{bmatrix} i_{m1} & v_{m1} \\ i_{m2} & v_{m2} \\ \dots & \dots \\ i_{mN} & v_{mN} \end{bmatrix} \begin{bmatrix} \frac{1}{C_m} + \frac{R_a}{R_m C_m} \\ -\frac{1}{R_m C_m} \end{bmatrix} \quad \text{or} \quad \mathbf{x} = \mathbf{A} \boldsymbol{\theta}$$

Form a least-squares estimator: $\hat{\boldsymbol{\theta}} = (\mathbf{A}^T \mathbf{A})^{-1} \mathbf{A}^T \mathbf{x}$

$$\text{where } \hat{\boldsymbol{\theta}} = \begin{bmatrix} \theta_1 \\ \theta_2 \end{bmatrix} \text{ and } \begin{bmatrix} R_m \\ C_m \end{bmatrix} = \begin{bmatrix} -\frac{\theta_1}{\theta_2} & -R_a \\ \frac{1}{\theta_1 + R_a \theta_2} \end{bmatrix}$$

Unfortunately, this method cannot be implemented on the current version of the Universal Clamp because of a problem associated with the intrinsic hardware of the front-end control board. The front-end control board uses the Blackfin BF548 Evaluation board, which uses direct memory access (DMA) to control the A/D converter and the D/A converter. As a result, the phase relationship between the injected current waveform and induced voltage waveform varies and cannot be precisely defined. The aforementioned vesicle detection algorithm requires the precise phase information. Thus, the front-end hardware of the Universal Clamp needs to be redesigned before the proposed time-domain method can be applied.

5.5 List of references

1. Nobelprize.org. The Official Web Site of the Nobel Prize. <https://www.nobelprize.org/nobel_prizes/medicine/laureates/2013/>. Retrieved in January, 2018.
2. Rituper B, Gucek A, Jorgacevski J, Flasker A, Kreft M, Zorec R. High-Resolution Membrane Capacitance Measurements For The Study Of Exocytosis And Endocytosis. *Nature Protocols* 8(6): 1170-83, 2013.
3. Allen JB. Short time spectral analysis, synthesis, and modification by discrete Fourier transform". *IEEE Transactions on Acoustics, Speech, and Signal Processing. ASSP-25* (3): 235–238, 1977.
4. Cooley JW. Lewis PAW, Welch PD. Historical notes on the fast Fourier transform.. *IEEE Trans. on Audio and Electroacoustics.* 15 (2): 76–79, 1967.
5. Sun Y, Scouten C. Method and apparatus for measuring electrical properties of cells. US Patent application no. 20150308973, filed April 2014.

CHAPTER 6

SYSTEMATIC TESTING OF THE UNIVERSAL CLAMP

6.1 Introduction

The Universal Clamp is the hardware platform to implement various digital signal processing tools for measuring and controlling the neuronal signals. Thus, this chapter summaries a systematic testing of the various functions of the Universal Clamp by use of a passive neuron model (3-element RC circuit) and the dynamic Neuron Emulator described in Chapter 3. The Universal Clamp was based on the Ph.D. thesis of Dr. Jiang Wu [1]. The present version of the Universal Clamp is the result of continuous improvement by Dr. Jiang Wu and Prof. Ying Sun.

6.2 Testing Setup

The setup of the Universal Clamp system requires a PC laptop. The operating system of the laptop should be either Windows 9 or Windows 10. The Universal Clamp and the laptop are connected via an Ethernet router. The router has an internal IP address of 192. 168.1.1. The front view of the system setup is shown in Figure 6.2.1 below. The front-panel on/off switch controls the power to the controller board. The green LED indicator labeled “Power On” is lit when the controller board is successfully turned on.

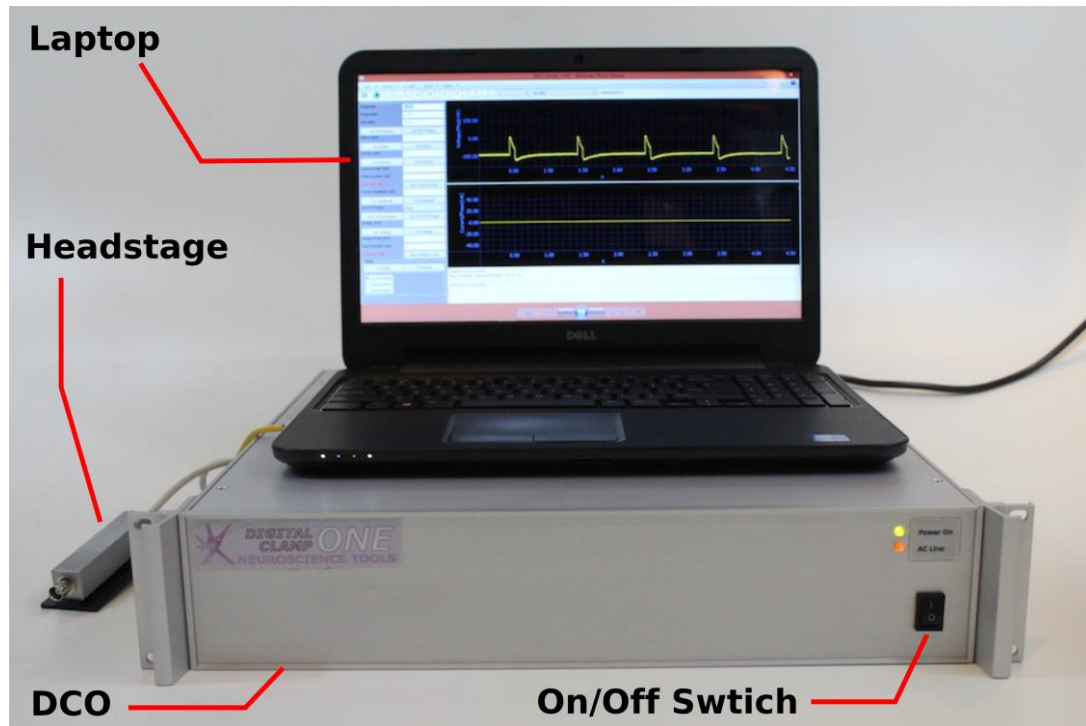


Figure 19 Testing Setup

The back view of the Universal Clamp setup is shown below. The following checklist shows the used connections.

1. The power cord was plugged to the Universal Clamp into a 120 VAC wall outlet. The on/off switch controls the power to the Universal Clamp unit including the built-in router. The orange indicator labeled “AC Line” on the front panel is lit when AC power is supplied to the unit.
2. The long RJ45 Ethernet cable was used to connect the laptop and the built-in router. any one of the 4 ports of the router could be used, but not the WAN port.

3. The short RJ45 Ethernet cable was used to connect the Universal Clamp and the router. any one of the 4 ports of the router could be used, but not the WAN port.
4. The headstage was connected to the 5-pin DIN receptacle on the back panel of the Universal Clamp labeled “headstage.” See Figure 6.3.2 for clarification!

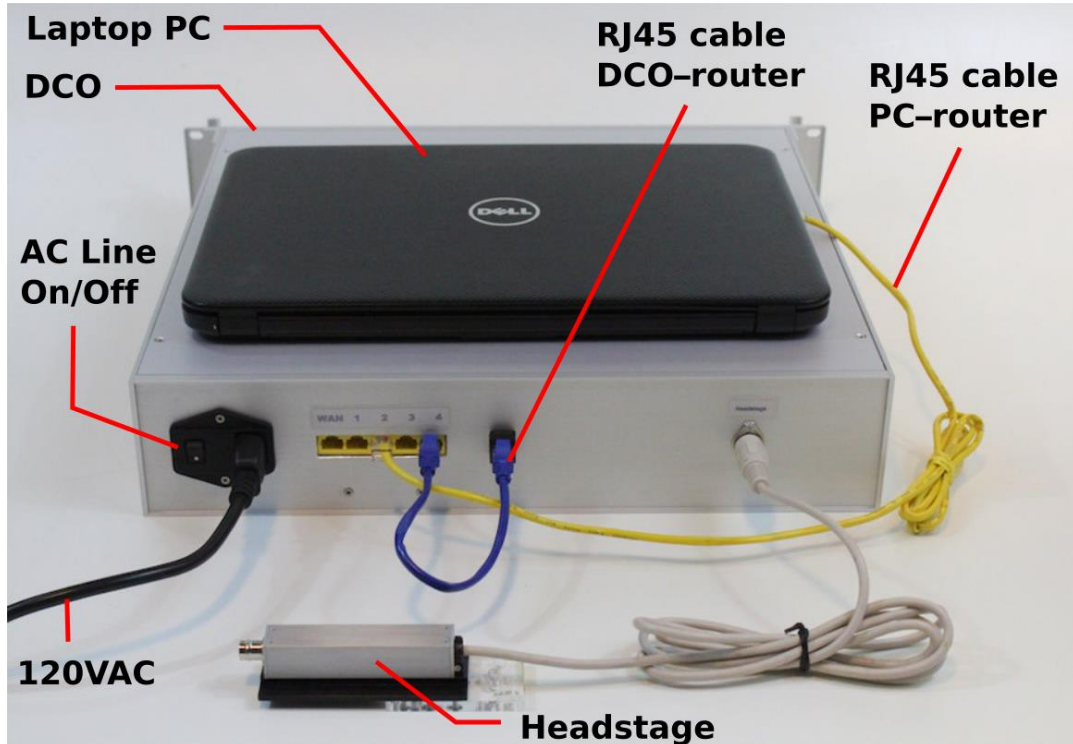


Figure 20 Back-panel view to illustrate the setup of the Universal Clamp

6.3 Ethernet Connection

By Plugging the power cord of the Universal Clamp to a 120 VAC wall outlet and turning on the back-panel power switch. The orange indicator on the Universal Clamp front panel (AC Line) should turn on. Turning on the front-panel power switch and the green indicator (Power On) should turn on. Launching the DCO_v104 program on the laptop. The instrument panel is shown in Figure 6.3.1 below.

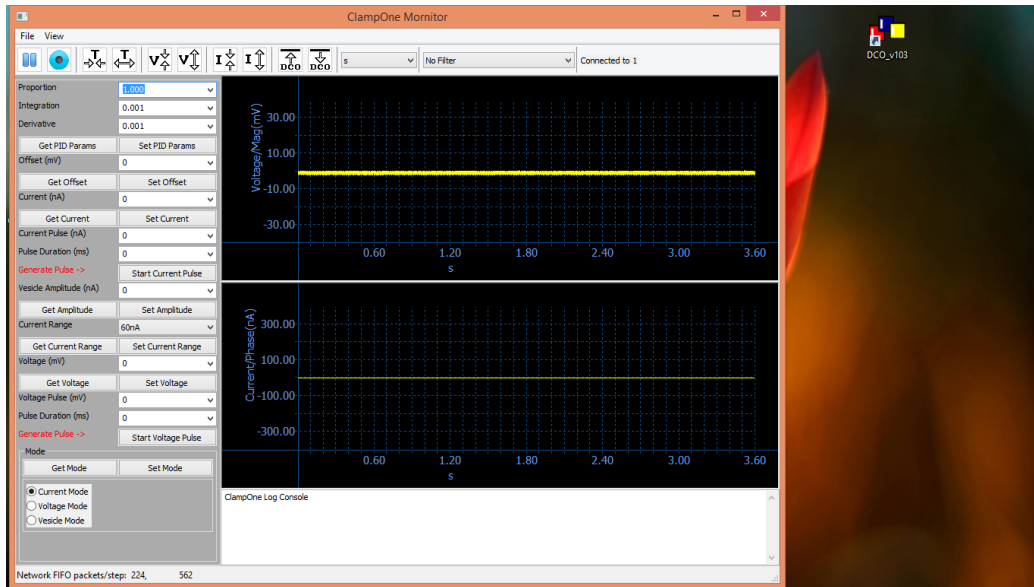


Figure 21 Instrument Panel

The “Connected to #” message should appear at the upper-right part of the screen. Every Universal Clamp controller board has been calibrated and assigned a unique identification number (#).

For testing purpose, the passive neuron model was inserted to the headstage as shown in Figure 6.3.2.

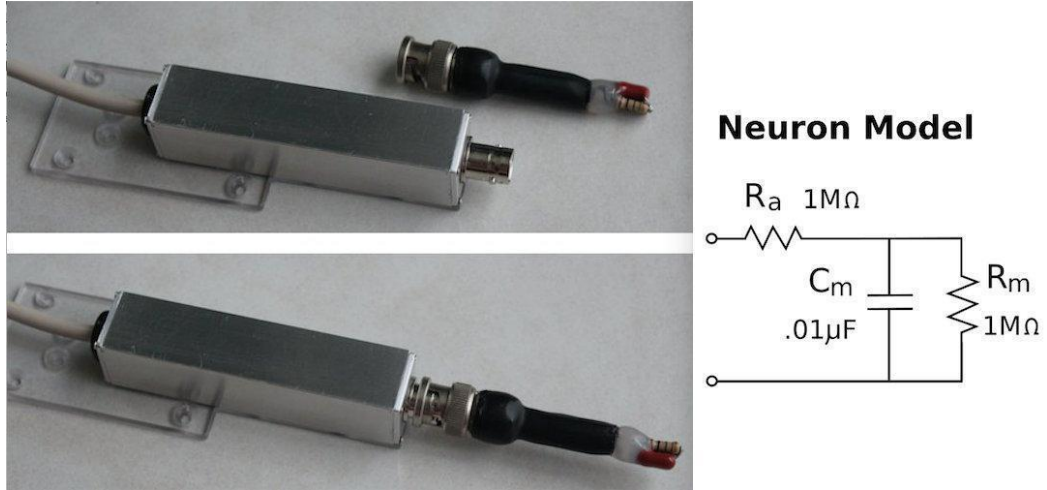


Figure 22 Passive Neuron Model & Headstage

The full-screen instrument panel is shown in the Figure below.

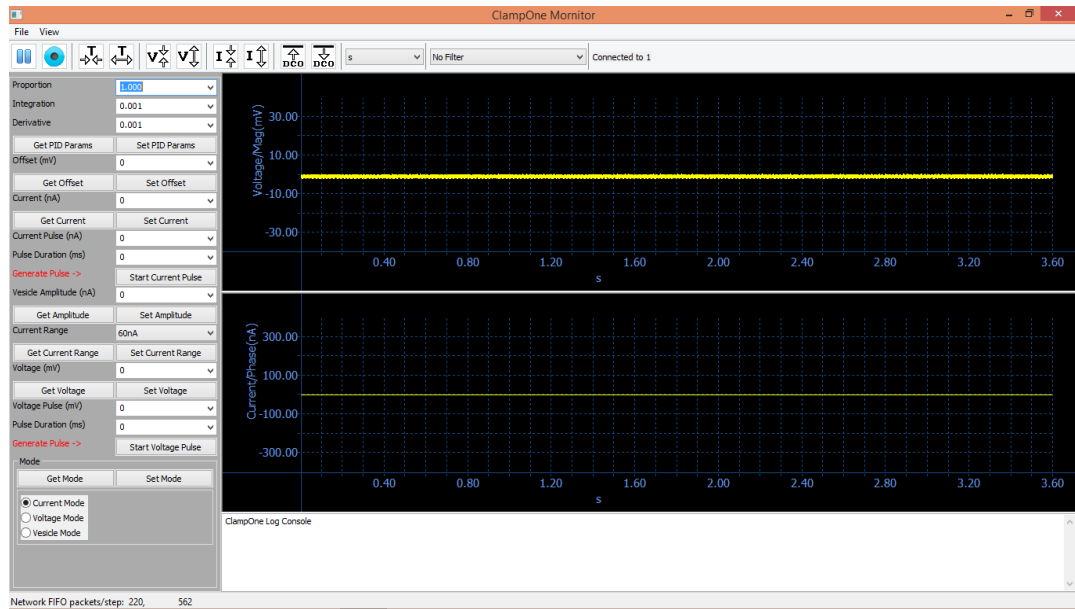


Figure 23 Full-screen Instrument Panel

At this point, data came in and was displayed in the voltage window (top) and the current window (bottom). Network activities were reported in the area below the current window.

The initial default mode was *current* clamp. The default current setting is 0 nA. Thus, the current trace was a noise-free flat line at 0. The voltage trace shows the intrinsic noise level and the offset voltage. The noise was mainly 60 Hz line noise picked up by the two 1 M Ω resistors of the neuron model. While it was relatively easy to remove this noise at the front-end control board by using the available filter bank, it was a good option to save the raw data and handle the noise problems with appropriate post-processing algorithms. This is because the front-end filter could remove essential components of the signal.

6.4 Instrument Panel

The user interface of the Universal Clamp is accomplished by a single instrument panel on the PC laptop as shown in Figure 6.4. The different sections and control buttons of the instrument panel are highlighted and explained below.

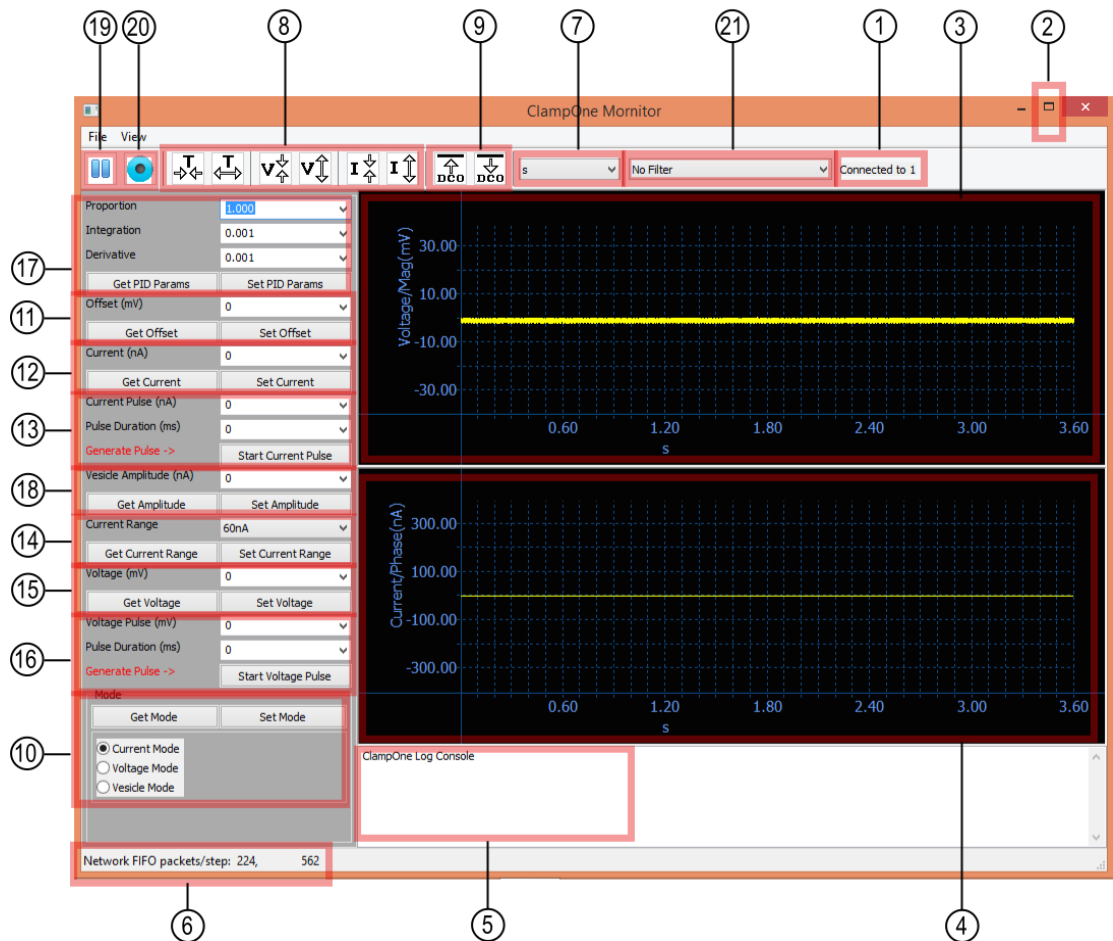


Figure 24 Instrument Panel

1. Network connection status:
 - a) “No connection” – means check the connection cables and make sure the Universal Clamp back-panel and front-panel power switches are turned on. If “Initialized network error: 18” appears in the Message Window (see 5), this is due to the non-termination of the network from a previous run of the software. Please either restart the PC or wait for few minutes and try again.

- b) “Connected to #” – This message indicates that the PC and the Universal Clamp are properly connected, where # is a unique ID number for the specific Universal Clamp controller board.
1. Full screen – This is the Windows option for expanding the window to full screen. The ESC key reverses from the full-screen mode to the standard mode.
 2. Voltage window – This window is used to monitor the voltage measurement in real time.
 3. Current window – This window is used to monitor the injection current in real time.
 4. Network activities – This is the message window that shows the activities of the network communications between the Universal Clamp and the computer.
 5. Packet queue status – The data from the Universal Clamp are segmented into packets. A queue is used to buffer the packets.
 6. Time axis unit – Click on the “V” mark to pull down the menu. The time unit can be s, ms, μ s, or point.
 7. Voltage, current, and time scales – These icons are used to expand/compress the voltage, current, and time scales. The waveforms can also be shifted up and down. This is accomplished by placing the cursor in the voltage or current window and use the scroll wheel on the mouse. If a touch pad is used, use the two-finger scroll.
 8. Parameters up/down-load – The “upload to computer from Universal Clamp” icon and the “download from computer to Universal Clamp” icon are used to coordinate all parameters of the display with the instrument. Either of these can

be clicked at any time. It is also used initially to establish the network connection between the Universal Clamp and the computer, if the connection does not happen automatically.

9. Voltage, current, capacitance modes – These buttons select the operational mode: current clamp, voltage clamp, or vesicle capacitance measurement. After a new mode is selected, click the *Set Mode* button to activate the Universal Clamp.
10. Set/get offset voltage – Enter the offset voltage for the electrode. For example, if the initial voltage baseline is 10 mV, enter -10 to cancel out the offset.
11. Set/get injection current – This is used for current clamp to send a constant injection current. Also, for vesicle mode, this current sets the baseline of the sinusoidal excitation for the capacitance measurement. The “V” mark activates a pull-down menu containing the previously selected values that can be re-entered.
12. Current pulse – This performs current clamp for a programmed duration. Enter the amount of current injection in nA and the duration of the pulse in ms. Click “Start Current Pulse” button. The Universal Clamp will send the current pulse and then return to initial current setting (see 12). The pulse duration is limited to 10 s (0–9999 ms).
13. Set/get current range – This sets the maximum current range to be either 6 nA, 60 nA, or 300 nA. A pop-up window will come out as a reminder for setting the hardware jumpers on the controller board. The current range cannot be set by software alone. The resistors on the controller board need to be changed and match the selected current range. See Section 13 Current Range for more details.

14. Set/get clamping voltage – This is used in the *Voltage Mode* to specify the command voltage for voltage clamp. The “V” mark activates a pull-down menu containing the previously selected values that can be re-entered.
15. Voltage pulse – This performs voltage clamp for a programmed duration. Enter the voltage amplitude in mV and the duration of the pulse in ms. Click “Start Voltage Pulse” button. The Universal Clamp will clamp to the desired voltage and then return to the initial voltage. The pulse duration is limited to 10 s (0–9999 ms).
16. Set/get PID controller parameters – These fields are used to set the gains for the proportional-integral-derivative controller for the voltage clamp. Generally speaking, the *Proportion* gain is the most sensitive and a higher gain can suppress oscillations. The *Integration* gain affects the accuracy of the DC voltage to be clamped to. The *Derivative* gain affects the fast transitions.
17. Vesicle Amplitude – During the *Vesicle Mode*, the cell capacitance is monitored continuously with a sinusoidal current injection. The baseline-to-peak value of the sine wave is set by the Vesicle Amplitude. The baseline is set by the Current field (see 12). The Current Pulse function (see 13) is still functional during the vesicle mode. Thus, it is possible to send a current pulse for a certain duration and observe the changes in vesicle activities.
18. Pause/play graphic display – This button is used to freeze/unfreeze the display.
19. Record/stop data to disk – This button controls the storage of data to a disk file called *record.dat* in the DCO_v104 folder.

20. Filter bank – The “V” mark activates a pull-down manual for choosing a desirable digital filter. See Section 7 Digital Filter Bank for more details.

6.5 Digital Filter Bank

Each filter was implemented as a 60 Hz notch filter combined with a low-pass filter. The choice of the cut-off frequency for the low-pass filter includes 1 KHz, 2 KHz, 3 KHz, 4 KHz, and 5 KHz, as shown. The filters were high-order finite-impulse-response (FIR) filters. They don't have a sharp cut-off response but are always stable and linear phase filters. See Figure 6.5.1 below.

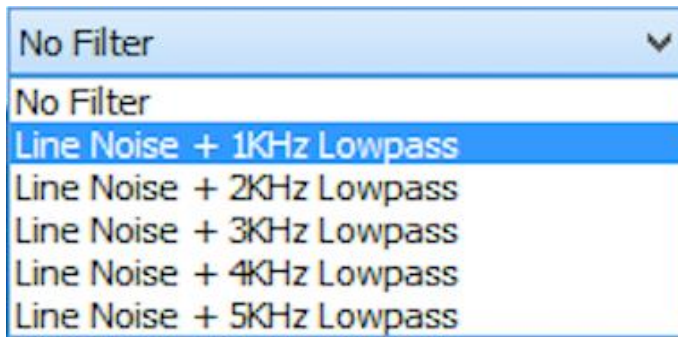


Figure 25 Digital Filter Bank

The example below in figure shows that the filter with the 1 KHz cut-off frequency reduces the noise level from 2 to less than 1 mV peak-to-peak.

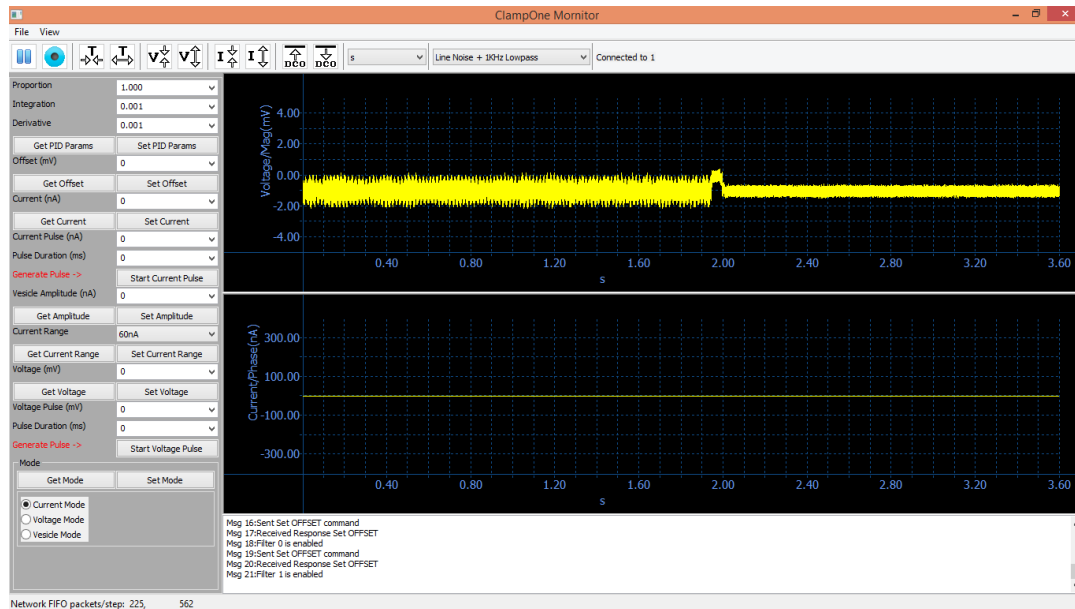


Figure 26 Filter with 1,000 Hz

6.6 Offset Voltage

Offset voltage was likely to exist due to the junction potential of the electrode setting. In this example the voltage trace shows an offset voltage of -0.8 mV. This offset voltage is removed by entering 0.8 in the *Offset (mV)* field and then clicking the *Set Offset* button, as shown in Figure 6.6. below.

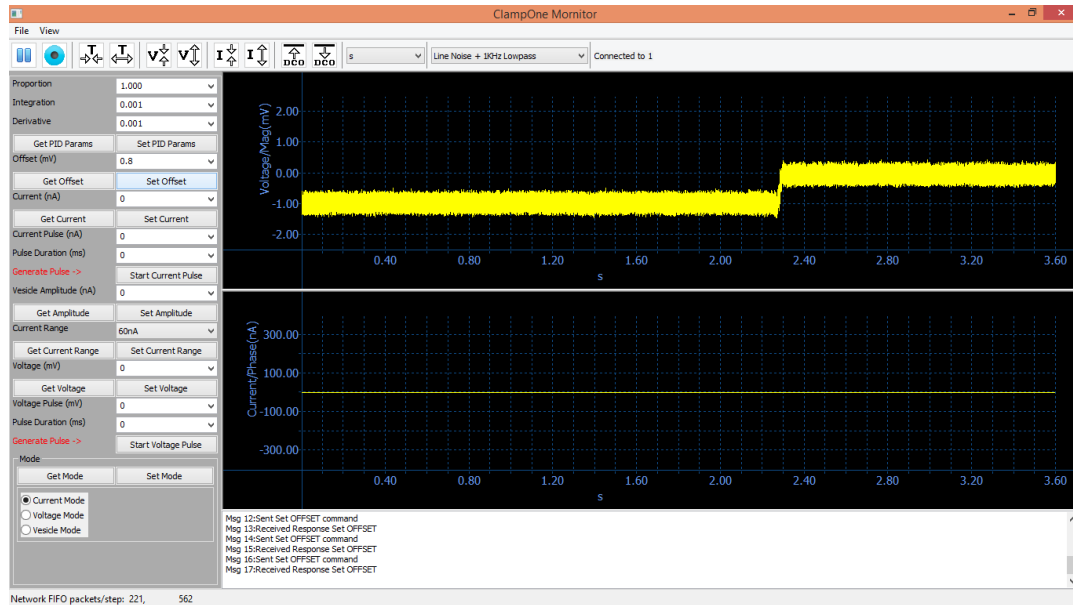


Figure 27 Offset Voltage

At any time, the *Get All* icon (Universal Clamp with up-arrow) could be clicked to retrieve all parameters from the Universal Clamp to ensure consistency between the instrument panel and the actual Universal Clamp setting. Conversely, the *Set All* icon (Universal Clamp with down-arrow) can be clicked to send all parameters shown on the instrument panel to the Universal Clamp.

6.7 Current Clamp

Current clamp is the default mode, as indicated by the *Current Mode* selection button. To set the injection current, enter the current in the *Current (nA)* field then click the *Set Current* button. For the example below, 10 nA is entered and the *Set Current* button is clicked. The current jumps to 10 nA and the voltage jumps to 20 mV. These values verify because the total resistance of the neuron model is 2 MΩ.

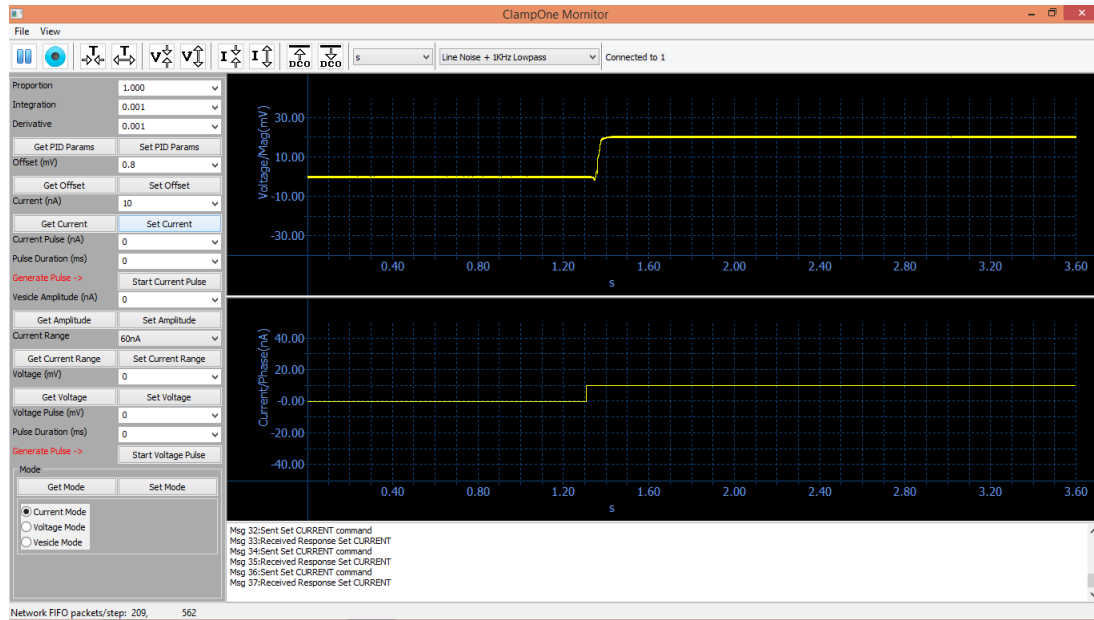


Figure 28 current jumps to 10 nA and the voltage jumps to 20 mV

Presently, there are 3 ranges for current injection: 6 nA, 60 nA, and 300 nA. The default is 60 nA, which means the maximum allowable current injection is 60 nA. To change the current range, not only the *Current Range* needs to be changed but also two specific jumpers on the circuit board needs to be changed. A attempt to change the current range results in a pop-up window as shown in Figure 6.7.2 below. This is to remind the testing user the jumpers on the circuit board inside Universal Clamp need to be set and match the current range setting.

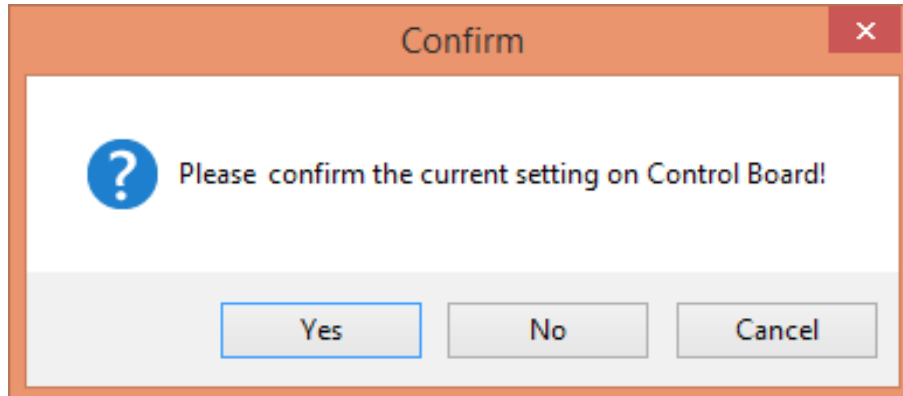


Figure 29 Message of current range setting

The Universal Clamp system allows for the generation of a current clamp pulse. This was accomplished by specifying the amplitude and the duration of the current clamp pulse. As shown in Figure 6.7.3 by the example below, the initial current clamp is set at 0 nA (no injection current). The *Current Amplitude* is set to 15 nA and the Pulse Duration is set to 1000 ms. After clicking the *Start Current Pulse* button, a current pulse is generated, and the voltage responds accordingly. After 1s the current returns to the initial value, which is 0 nA in this case.

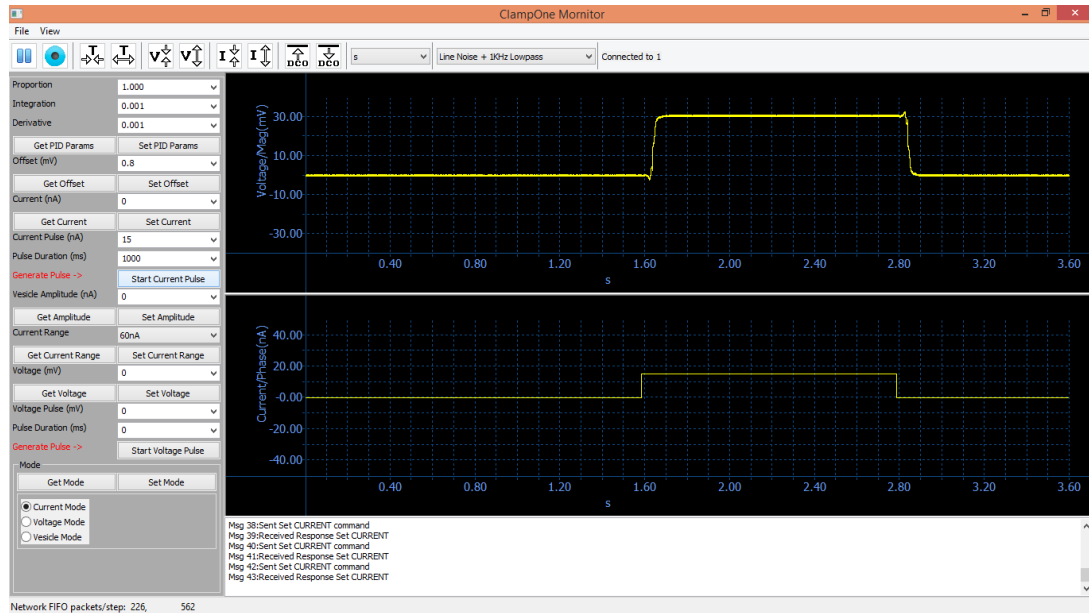


Figure 30 Injection a current pulse

6.8 Voltage Clamp

To perform voltage clamp, Select the *Voltage Mode* button and click the *Set Mode* button. The example in Figure 5.8.1 above shows a voltage clamping to 30 mV. Because the load is the passive neuron model (2 M Ω), the required current injection is 15 nA after the initial transient.

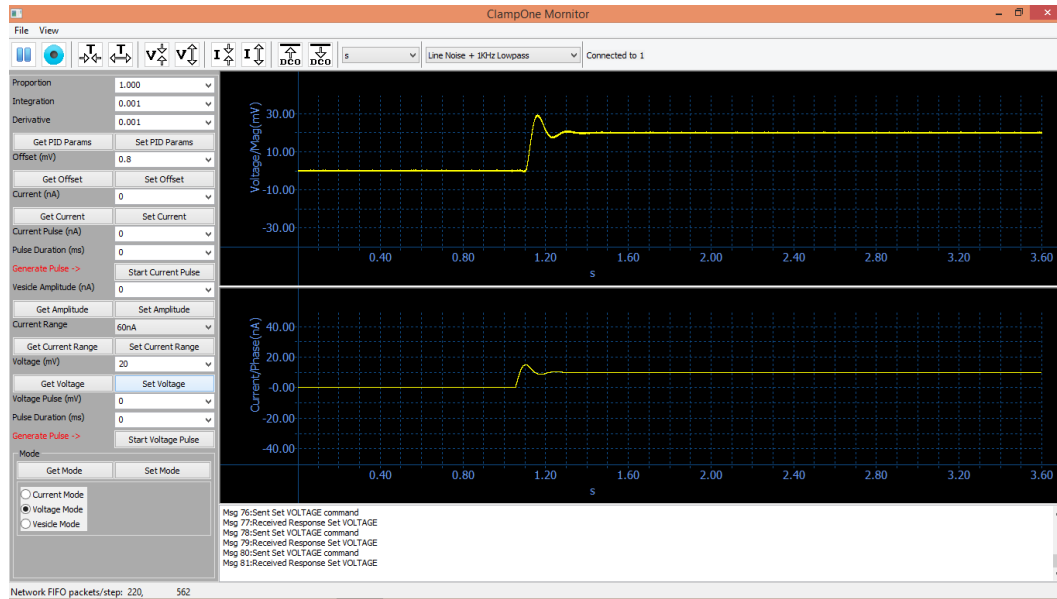


Figure 31 Voltage Clamp Example

The feedback control of the voltage clamp is accomplished with a proportional-integral-derivative (PID) controller, which is implemented by the digital signal processor. The default PID gains are set at: $P = 1.0$, $I = 0.001$, and $D = 0.001$. Generally speaking, the P gain is the most sensitive parameter on the PID controller's performance. The integral gain can further control the error at the DC level. The derivative gain can further improve the response at higher frequencies.

The desirable PID gains can be entered and then downloaded to the Universal Clamp by clicking the *Set PID Params* button. For example, in order to suppress the initial oscillation of the voltage clamp shown above, the *Proportion* gain is changed to $P = 5.0$. The result in Figure 6.8.2 below shows a reduction of oscillation and a significant shorter settle time at the onset of the voltage clamp.

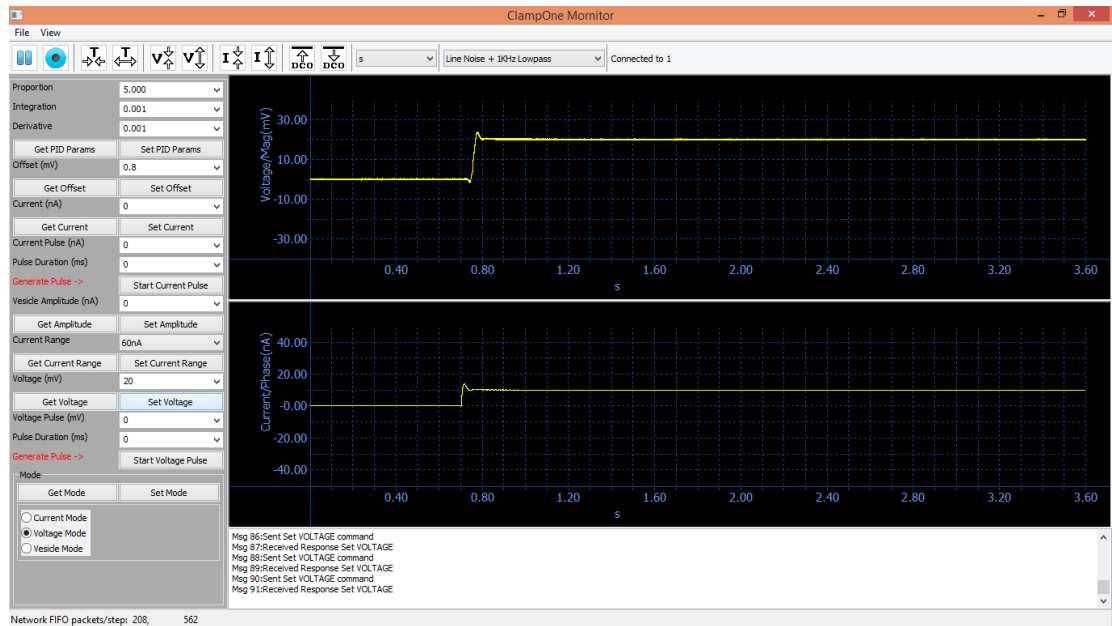


Figure 32 Voltage clamp on the passive neuron model with an increased Proportion gain ($P=5.0$), which resulted in a reduction of oscillation and a significant shorter settle time at the onset of the voltage clamp

6.9 Voltage Clamp with Neuron Emulator

This section describes an advanced test of the voltage clamping performance by use of an active neuron emulator. As described in Chapter 3, the Neuron Emulator uses a switching circuit to generate action potentials of a fast rise time. This neuron emulator has both passive and active electrical properties very similar to those of a live neuron. The connection of the head stage to a prototype neuron emulator circuit is shown in the Figure.

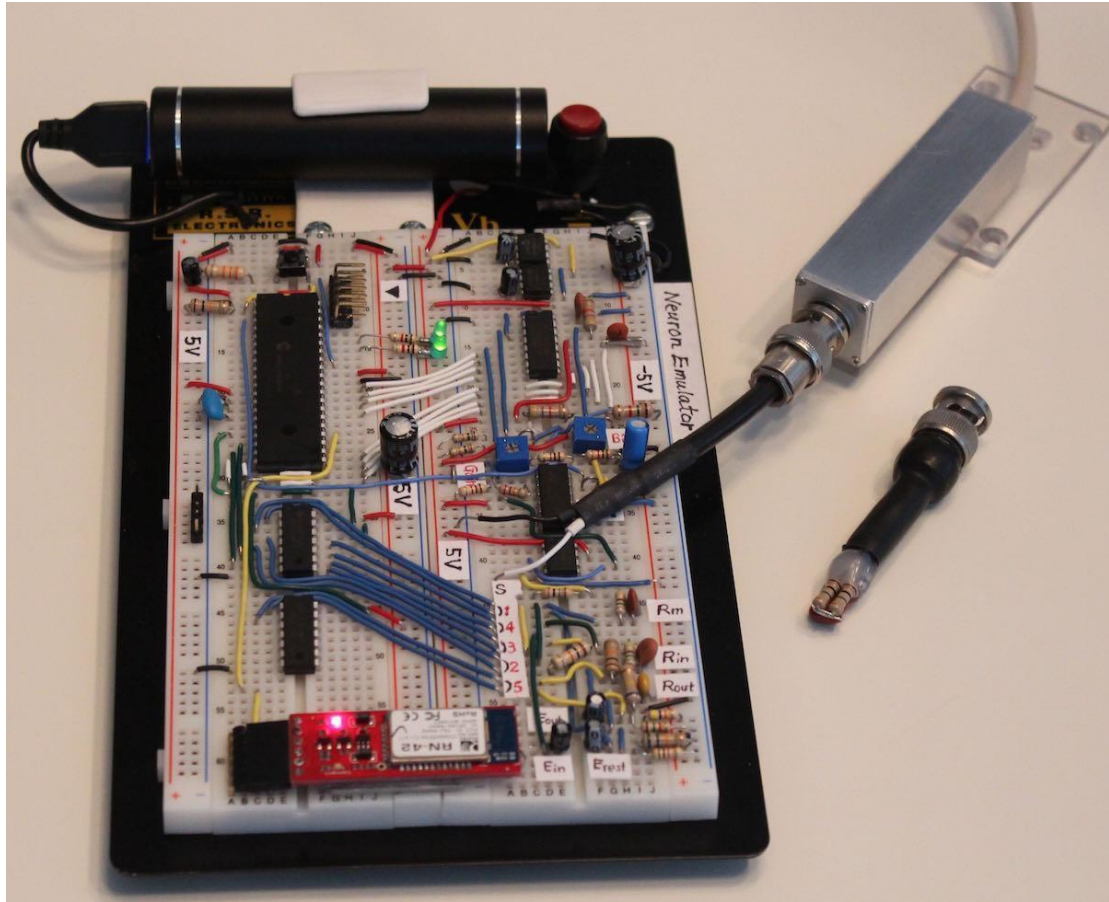


Figure 33 Neuron Emulator circuit with the connection to the headstage

The result of the voltage clamp experiment with the active neuron emulator is shown in Figure below.

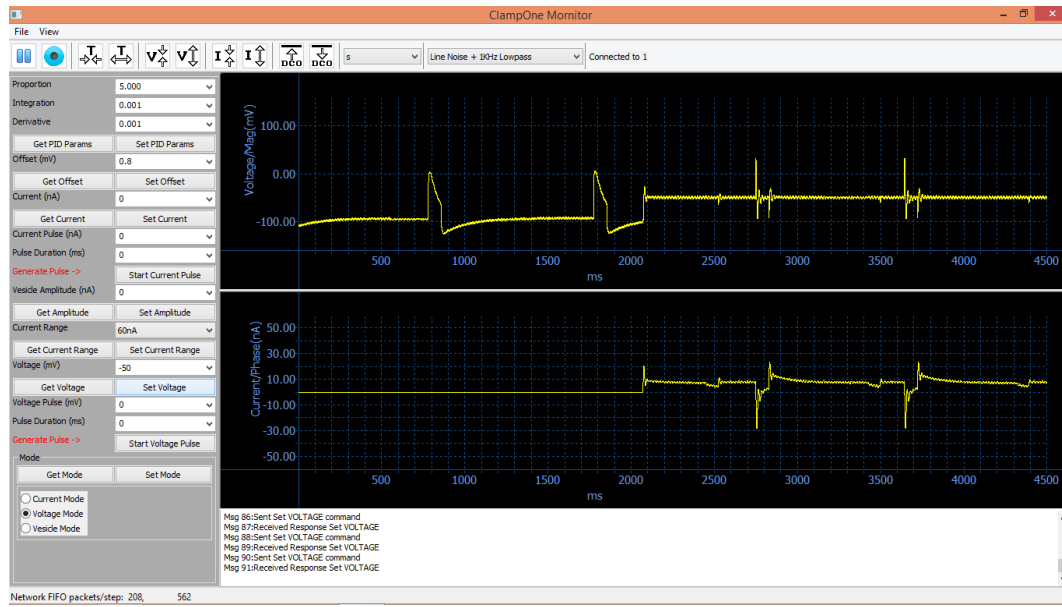


Figure 34 result of the voltage clamp experiment

As shown in the voltage window, after the first two action potentials on the left, the voltage clamp is turned on. The voltage was clamped to the baseline at -95 mV. For the most part the action potentials are nullified, with the exception of the fast rises and falls of the spikes. The current waveform correctly shows the inward and outward current components that are used to generate the action potentials.

The rise and fall of the spikes from this neuron emulator are at least 10 times faster than those from the real neurons. Thus, the response time of the Universal Clamp system for voltage clamping is considered adequate.

6.10 Voltage Clamp With Modified Neuron Emulator

As described in Section 3.5.2, an attempt to slow down the initial rise time of the action potential generator by the Neuron Emulator was proposed by adding a low-pass filter at the output. The resulting action potential has a rise time on the order of 1 ms and better resembles a real action potential, as shown in Figure 6.10.1.

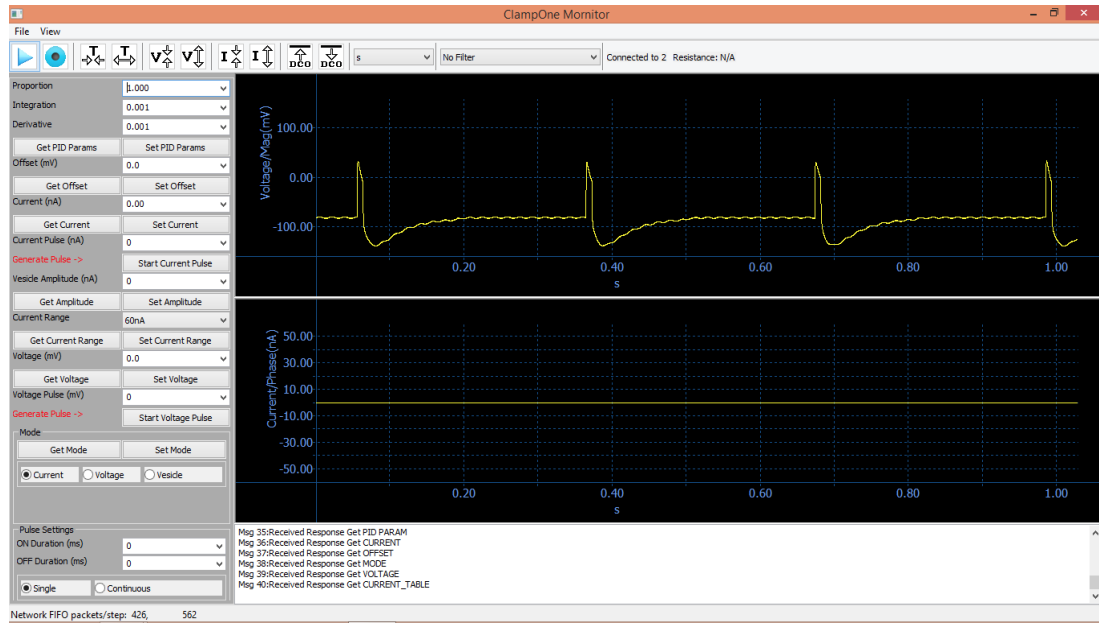


Figure 35 Action potentials generated by the modified Neuron Emulator with a low-pass filter added to the output

However, the RC circuit also interfere with the feedback control during voltage clamp. As shown in Figure 6.10.2, the voltage clamp was unsuccessful with the *Proportion* gain set to $P = 1.0$. The situation was slightly improved by increasing the *Proportion* gain to $P = 5.0$, as shown in Figure 6.10.3.

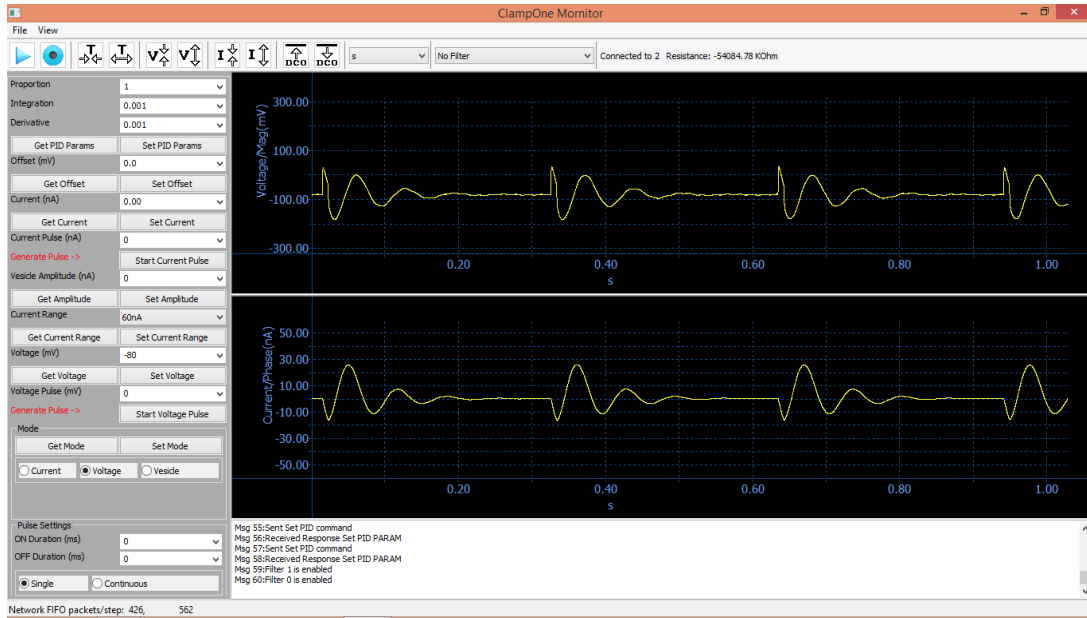


Figure 36 Unsuccessful voltage clamp with the modified Neuron Emulator that has an added RC circuit at the output (Proportion gain = 1.0)

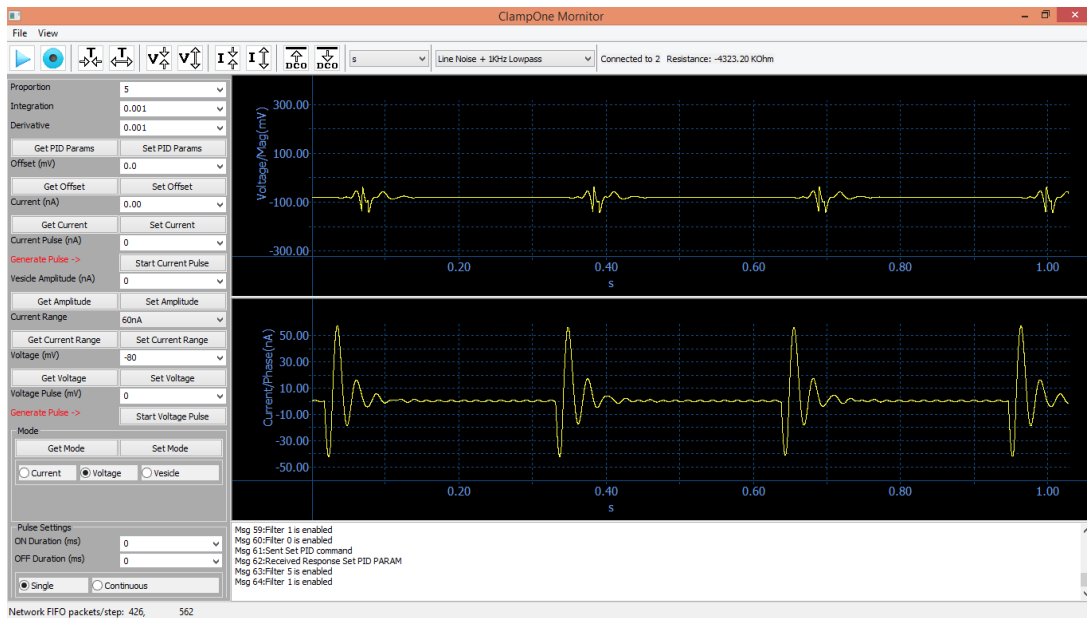


Figure 37 Slightly improved voltage clamp with the modified Neuron Emulator that has an added RC circuit at the output (Proportion gain = 5.0)

With a higher time resolution in Figure 6.10.4, the delay of the feedback current can be observed, which explains the failure of the voltage clamp.

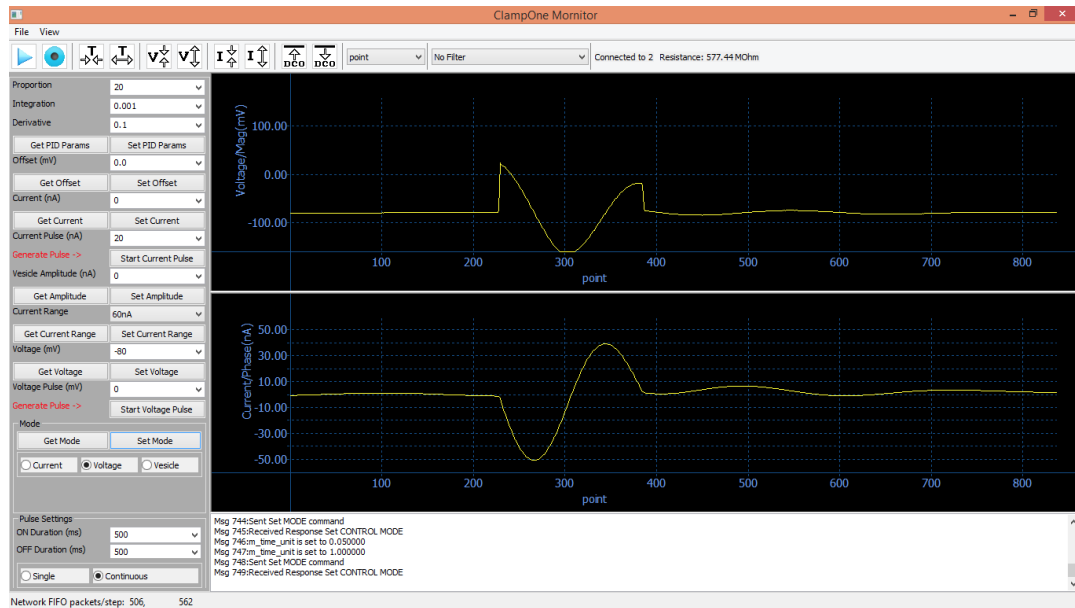


Figure 38 With a higher time resolution the delay of the feedback current can be observed

In summary, the attempt to reduce of the rise time of the action potential spike by adding a low-pass filter at the output circuitry does make the action potential waveform more realistic. However, the low-pass filter also reduces the speed for the feedback currents and results in an unsuccessful voltage clamp.

6.11 List of References

1. Wu J. Instrumentation in neurophysiology and modeling in biochemistry. Ph.D. dissertation, Department of Electrical, Computer and Biomedical Engineering, University of Rhode Island, 2004.

CHAPTER 7

TESTING OF CELL CAPACITANCE MEASUREMENTS

7.1 Instrumentation

The figure shows the block diagram of the instrumentation system for testing the cell capacitance measurements. The Cell Capacitance Emulator (CCE) has two outputs. The “RC output” is sent to the Universal Clamp. The “C output” is sent to the capacitance meter (Model 3000, GLK Instruments, San Diego, CA) for determining the precise capacitance values. The capacitance meter also has an analog output, which is displayed on an oscilloscope.

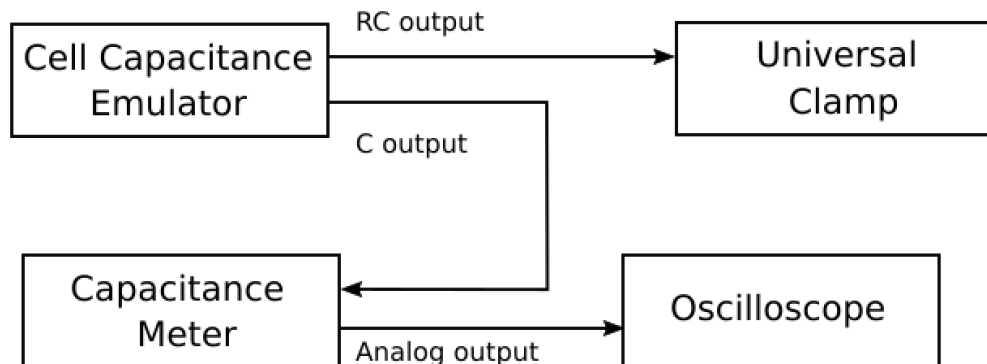


Figure 39 Block diagram of the instrumentation system for testing the cell capacitance measurements

The operation on the Universal Clamp is as follows. By electing the *Vesicle Mode* and then clicking the *Set Mode* button to operate in the capacitance measurement mode. A sinusoidal current waveform was used to excite the neuron for

the capacitance measurement. The baseline-to-peak amplitude of the sinusoidal wave is set by use of the *Vesicle Amplitude* field and the baseline by the *Current* field. See *Section 6.7 Current Clamp* for more details. The current amplitude should be set at a large value for increasing the signal-to-noise ratio. But too large an amplitude may have undesirable effects such as triggering the action potentials. It is also possible to use the current pulse mode such that the baseline of the sinusoidal wave can change during the pulse duration.

7.2 Test Results

The voltage window now shows the magnitude of the frequency response, and the current window shows the phase of the frequency response. The detection of the vesicle activities can be based on either the magnitude and the phase. In general, the phase should be more sensitive than the magnitude. The result in Figure 7.2.1 below shows a simulation of the vesicle detection by touching the passive neuron model with fingers intermittently. The *Vesicle Amplitude* is set to 10 nA. The baseline of the sinusoidal wave is 10 nA, changes to -10 nA for 8 s, and returns to 10 nA.

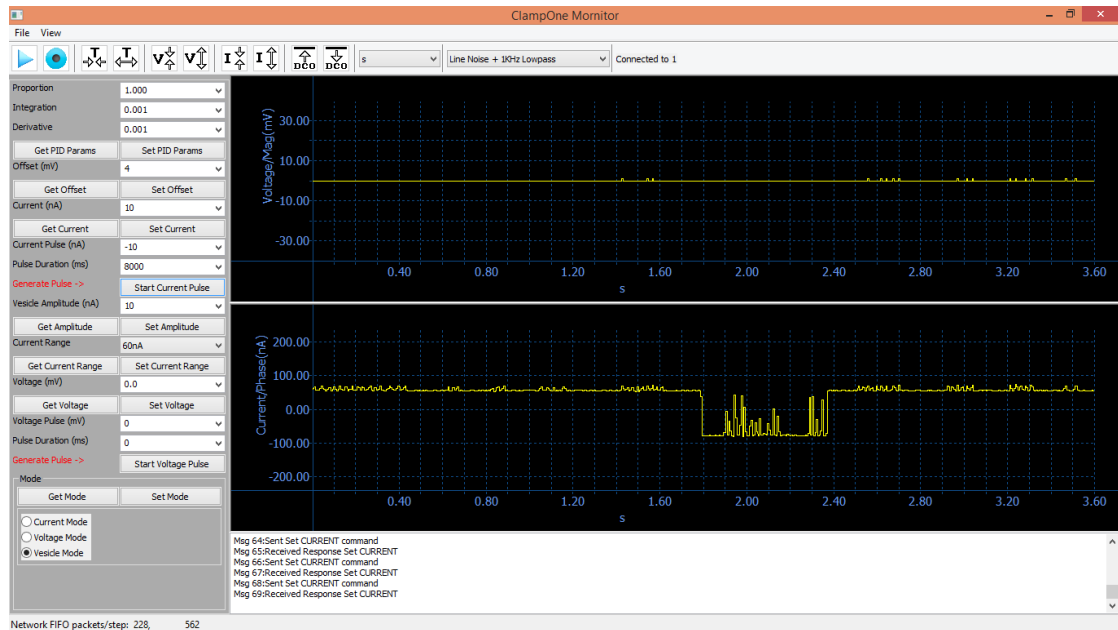


Figure 40 Vesicle detection with the finger touching the passive neuron model

The next test is to use the CCE for presenting the dynamic capacitance changes. The setup is according to Figure 7.1. The capacitors of the CCE are chosen such that the C output changes between 24.2 pF and 24.7 pF. This represent a capacitance change of 500 fF, which is about 50 times larger than the typical capacitance change due to a single vesicle activity. The capacitance pulse width is set to 500 mS, which is about 250 times wider than the actual vesicle pulse width. Nevertheless, the present algorithm was not sensitive enough to detect the pulses. Both the magnitude and the phase show no activities as shown in the Figure.

The experiment is repeated with a large capacitance to make sure there is no other instrumentation issue. A 10 nF capacitance difference is introduced. As shown in the figure, the Universal Clamp is capable of detecting the pulses with pulse width set to 200 ms, 50 ms, 10 ms, and 2 ms, respectively.

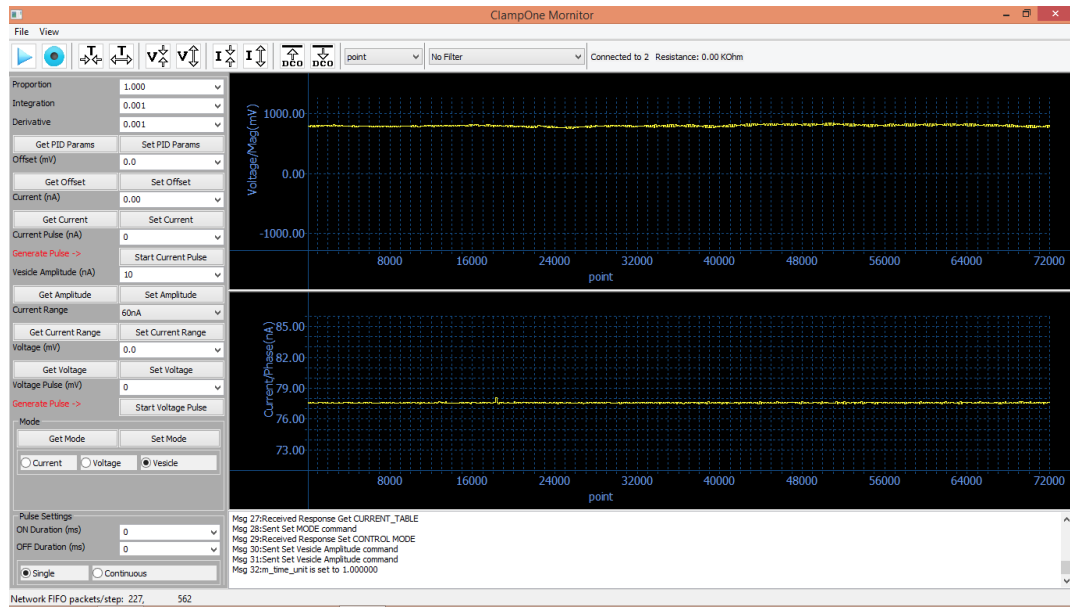


Figure 41 The present algorithm in the Universal Clamp failed to detect vesicle capacitance pulses with a 500 fA capacitance change and 1 500 mS pulse width

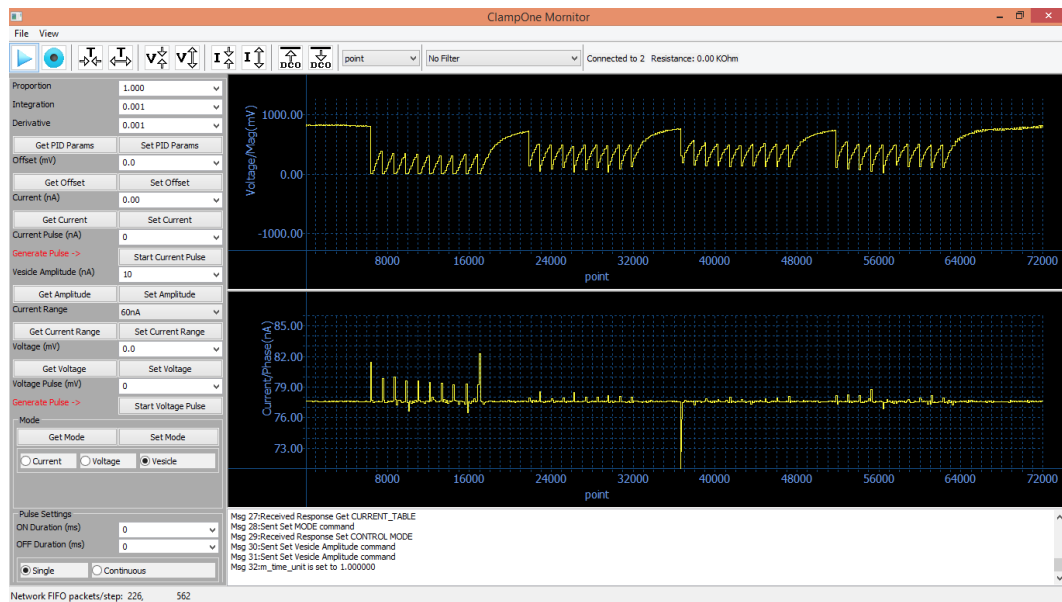


Figure 42 With a 10 nF capacitance difference, the Universal Clamp is capable of detecting the pulses with pulse width set to (left to right) 500 ms, 200 ms, 50 ms, and 2 ms, respectively

The GLK Model 3000 is the most sensitive capacitance meter available on the market. Thus, its performance can be considered as the state-of-the-art standard. The 500 fA pulses are presented to the capacitance meter. As shown in Figure 7.2.4, the capacitance meter is capable of detecting the 500 fF pulses with the 200 ms pulse width (left), but not with the 50 ms pulse width (right).

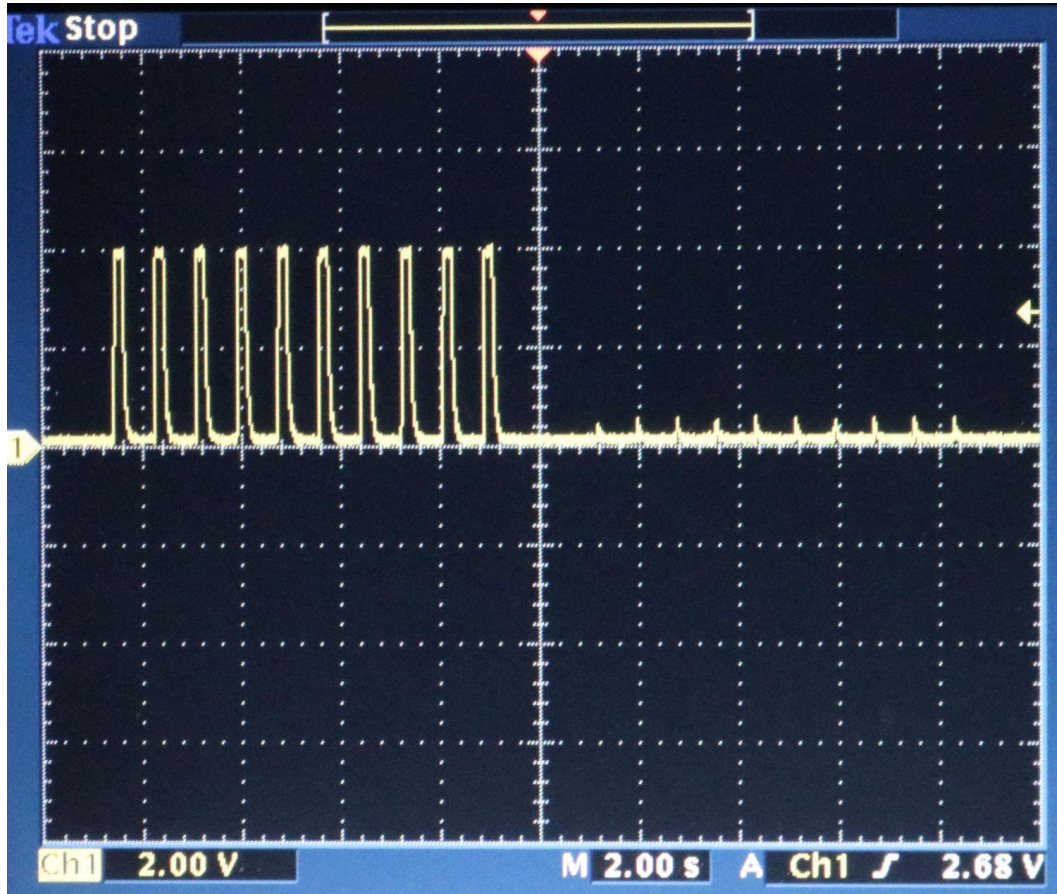


Figure 43 The capacitance meter (GLK Model 3000) is capable of detecting the 500 fF pulses with the 200 ms pulse width (left), but not with the 50 ms pulse width (right)

The specifications of GLK Model 3000 indicate that the analog bandwidth depends on the selected range [1], as shown in Table.

Table 2 Analog bandwidths for difference selected ranges of the capacitance meter (GLK Model 3000)

Selected Range	Analog Bandwidth	Time Resolution
2 nF, 20 nF, 200 nF	64 Hz	16 ms
200 pF	15 Hz	92 ms
20 pF	2.8 Hz	357 ms
2 pF	1.2 Hz	833 ms

The range selected for the above measurement is 200 pF, which has a time resolution of 92 ms. This explains why the capacitance meter can measure capacitance pulses with the 200 ms pulse width, but not the 50 ms pulse width.

In summary, the representation of the cell capacitance change due to a vesicle activity on the order of 10 fF with a 2-ms pulse width was challenging. The parasitic capacitance from the wiring and the breadboard was often on the order of 10 pF. The existing algorithm based on short-time Fourier transform for detecting the vesicle capacitance was insufficient to detect such a small and fast capacitance change. Nevertheless, the proposed instrumentation system based on the cell capacitance

emulator for testing the measurement of capacitance pulses is very useful. It is relatively easy to set up and provides qualitative as well as quantitative results.

7.3 List of References

1. GLK Instruments. Model 3000 Digital Capacitance Meter: Operation and CalibrationManual, version 3.3. <http://www.glkinst.com/cmtrdocs/Instruction%20and%20Service%20Manual_revision_3.3.pdf>. Retrieved in October 2017.

BIBLIOGRAPHY

- Allen JB. Short time spectral analysis, synthesis, and modification by discrete Fourier transform". IEEE Transactions on Acoustics, Speech, and Signal Processing. ASSP-25 (3): 235–238, 1977.
- Breau F, Maio-Cannon S, Davis R, Wu J, DiCecco J, Sun Y. The neuron emulator: an undergraduate biomedical engineering design project. 31st Annual Northeast Bioengineering Conference, Hoboken, NJ, pp. 29-30, April 1-3, 2005.
- Cooley JW, Lewis PAW, Welch PD. Historical notes on the fast Fourier transform.. IEEE Trans. on Audio and Electroacoustics. 15 (2): 76–79, 1967.
- Excel Cell Electronic Co., Taiwan. EDR202A0500 DIP Reed Relay Datasheet. <<https://www.digikey.com/products/en?keywords=edr202>>. Retrieved in October 2017.
- GLK Instruments. Model 3000 Digital Capacitance Meter: Operation and Calibration Manual, version 3.3. <http://www.glkinst.com/cmtrdocs/Instruction%20and%20Service%20Manual_revision_3.3.pdf>. Retrieved in October 2017.
- Hoffman K, Tran V, Blandin J, Wu J, & Sun Y. An Electronic Neuron Emulator that Models Inward and Outward Membrane Currents. 42nd Ann Northeast Bioengineering Conference, SUNY Binghamton, Vestal, NY, April 5-7, 2016.

Purves D, Augustine GJ, Fitzpatrick D, Katz LC, Anthony-Samuel LaMantia AS, McNamara JO, and S Mark Williams SK (editors). Sunderland (MA): Sinauer Associates, ISBN-10: 0-87893-742-0, 2001.

Rosenberg L, Hammick M, Sladen S, Wang T, Wu J, & Sun Y. An Electronic Model for Vesicle Induced Cell Membrane Capacitance Changes. 42nd Ann Northeast Bioengineering Conference, SUNY Binghamton, Vestal, NY, April 5-7, 2016.

Semiconductor Components Industries, LLC. MC14066B Quad Analog Switch/Quad Multiplexer (Rev. 3). On Semiconductor, <http://onsemi.com>, March, 2000.

Sun Y, Wu J, Collis L, Hill RB. Apparatus for neuromuscular measurement and control. Patent no. US 7,489,965 B2, February 10, 2009.

Sun Y, Wu J, DiCecco J, Hill RB. Processor controlled voltage-current analysis of nerve and muscle tissues. Patent no. US 8,000,783 B2, August 16, 2011.

Sun Y, Rieger R. Apparatus for memristor/neuron emulation and testing. Patent no. US 8,990,137 B2, March 24, 2015.

Wu J. Instrumentation in neurophysiology and modeling in biochemistry. Ph.D. dissertation, Department of Electrical, Computer and Biomedical Engineering, University of Rhode Island, 2004.

Wu J, DiCecco J, Sun Y, Hill R. An analog neuron emulator for education and testing of neurophysiological instruments. Society for Neuroscience 34th Annual Meeting, San Diego, CA, October 23-27, 2004.

Wu Y, Chen J, Rieger R, & Sun Y. A Neuron Emulator for Signal-Electrode Settings. 37th Ann Northeast Bioengineering Conference, Rensselaer Polytechnic Institute, Troy, NY, April 1-3, 2011